CDF/ANAL/TRIGGER/CDFR/9954
Version 1.0
October 6, 2009

Study of Multijet Triggers for all-hadronic Higgs search

Ankush Mitra,Shang-Yuu Tsai,Song-Ming Wang [1]

Institute of Physics - Academia Sinica, Taipei, Taiwan

Abstract

The note describes the study of multijet triggers for the all-hadronic Higgs search. It is an update of the previous trigger analysis used for the 2 fb^{-1} analysis. This note includes the results of new L2-CONE clustering and the new VH_MULTIJET trigger. In addition to studying the new Level-2 clustering algorithm & new trigger, a new method to apply the MC corrections has been developed which improves the agreement between simulation and data.

Contents

[1] mitra@fnal.gov,sytsai@fnal.gov, smwang@fnal.gov

1 Introduction

The Higgs boson remains as the only undiscovered particle of the Standard Model of particle Physics. At CDF, there are many analyses which are conducting searches for the Higgs in a variety of decay modes. The most sensitive channels are leptonic channels. This gives a search channel with low backgrounds but they all suffer from low event yields. The all hadronic analysis exploits the hadronic decay modes which has the largest cross-section $\times$ branching-ratio. The two production modes which will be studied in this analysis are shown in figure 1. The final state consists of 4 high-pT jets; two are b-jets and the other two are non-b jets.

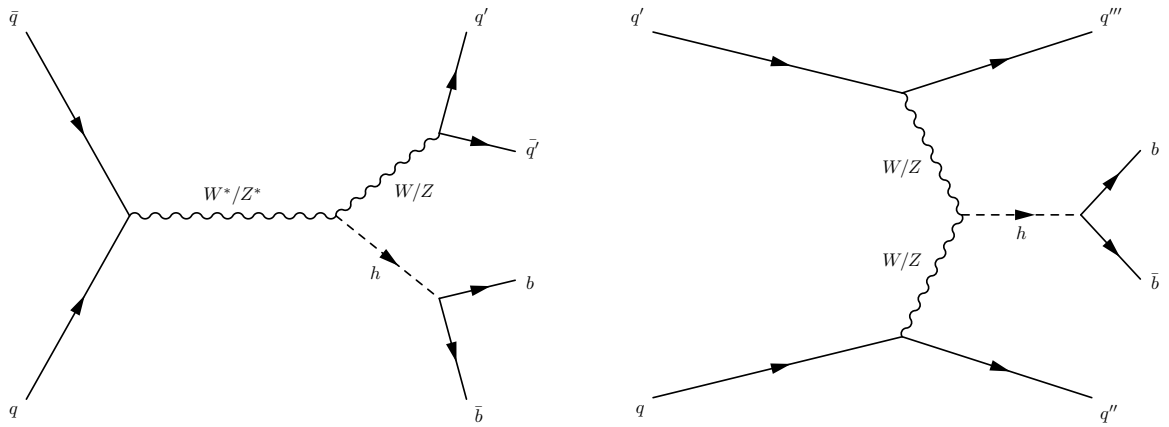

(a) Associated W/Z Higgs production.

(b) Vector Boson Fusion

Figure 1: Higgs productions modes with $b\bar{b}q\bar{q}$ final states. Both of these production modes are to be studied in the latest all-hadronic Higgs search.

In 2008, an all-hadronic analysis was blessed using 2 fb^{-1} of data [1]. This note is an update on the trigger study of that analysis [2]. Since the 2 fb^{-1} study, two major changes to the trigger took place:

- After Period-13, the L2 clustering algorithm changed from PACMAN to L2-CONE [3].
- The new VH_MULTIJET trigger was added during Period-18 to improve the acceptance for low- mass Higgs signals [4].

As part of the trigger study, the methods used to correct the simulation were reviewed. A new method was developed which further improved the CDF simulation match to data.

2 The Multijet Triggers at CDF

The signature for the all-hadronic Higgs channel are 4 high-P_T jets with large Sum-Et [2] . The TOP_MULTI_JET and VH_MULTIJET multi-jet triggers are designed to select events

[2] Sum-Et: Scalar Et sum of jets

with these signatures. At CDF, there are two standard ways of studying triggers:

- Cut on a parameter where the trigger is fully efficient.
- Measure the trigger turn-on from data and use it to weight the MC.

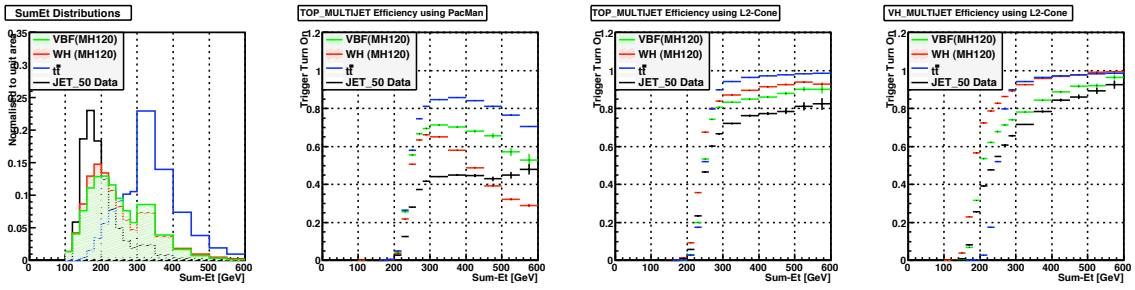

Figure 2: The left plot shows the Sum-Et distributions for Higgs Signals, JET_50 data (QCD), and $t\bar{t}$. The following three plots are the trigger efficiencies for TOP_MULTI_JET and VH_MULTIJET triggers. The graphs shows the trigger response is sensitive to the event topology and clustering algorithm. NB: Non-linear bining has been used for these plots.

Figure 2 illustrates why neither of the standard methods can be applied to the all- hadronic Higgs search. If one were to select events where the trigger has reached a plateau (Sum-Et $\gtrsim$ 300 GeV), the efficiency for Higgs events would be very small. Contrast this with $t\bar{t}$ where the Sum-Et spectrum is much harder, so a simple SumEt would be sufficient. The other approach of measuring the trigger turn-on from data cannot be applied as both multi-jet triggers are sensitive to the event-topology. Thus one must rely on CDF simulation to estimate the trigger turn-on. But one must ensure the CDF simulation correctly reproduces the multi-jet trigger. The previous trigger study had shown the trigger turn-on can be factorised into two components: PHYSICS & DETECTOR.

PHYSICS The jet-Et and Sum-Et distributions of the MC sample must match the distributions measured with data.

DETECTOR The energy of L2 clusters from MC and data must match.

After these corrections, any difference can be attributed to the differences between the details of the CDF simulation and recorded data. This remaining *scale factor* is applied to MC to get the correct trigger response.

3 Datasets used & Event Selection

Throughout this trigger study, all events were required to pass the *Standard Event Selection* which is defined below:

- Event is from a Good-Run (defined from Good-Run-List V27 (QCD+Silicon)

- $|Z_{Vertex}| < 60$ cm for highest-P_T vertex
- Lead Jet-Et > 60 GeV
- The event has at least 4 jets where a jet is defined as:
  - Cone 0.4 jets
  - Raw Jet-Et > 10 GeV
  - Level 7 corrected Jet-Et > 15 GeV
  - $|\eta| < 2.4$

For this trigger study, the data-sets used are:

- JET_50 Data – Period 0 to Period 20
- QCD-MC Pt40 (bt0srb and bq0src)

Throughout the text, Sum-Et (All Jets) is used to parameterise the trigger turn-on. This variables is defined as:

$$\text{Sum-Et(All Jets)} \equiv \text{Sum over all jets with Et} \geqslant 15\,\text{GeV}$$

4 The Reweigh Matrix

As the multi-jet triggers are sensitive to the event topology, it is important to match the input jet Et and angular distributions when comparing MC to data. In the previous trigger analysis note, an iterative procedure was applied to match the MC to the data. In this note, a *Reweigh Matrix* [3] was applied to match the MC to data. This has the advantage of not only reproducing the jet distributions but it also accounts for any correlations between jets. The added advantage is the *Reweigh Matrix* can be derived in a single pass. The *Reweigh Matrix* is defined in equation 1.

$$\begin{aligned}\text{Reweigh Matrix}&[Jet1-Et][Jet2-Et][Jet3-Et][Jet4-Et][Sum-Et][MIN\Delta R(4-jets)]\\ &= \frac{\text{Data}[Jet1-Et][Jet2-Et][Jet3-Et][Jet4-Et][Sum-Et][MIN\Delta R(4-jets)]}{\text{MC}[Jet1-Et][Jet2-Et][Jet3-Et][Jet4-Et][Sum-Et][MIN\Delta R(4-jets)]}\end{aligned} \quad (1)$$

Each dimension of the *Reweigh Matrix* is defined below:

$Jet1-Et$ Leading Jet Et

$Jet2-Et$ Second Leading Jet Et

$Jet3-Et$ Third Leading Jet Et

[3] The reweigh matrix was inspired by the Tag-Rate-Function method used to predict the QCD background in the 2fb^{-1} analysis.

$Jet4 - Et$ Fourth Leading Jet Et

$Sum - Et$ Scalar sum of all jets with Raw-Et>10 GeV & L7-Corrected Et >15 GeV

$MIN\Delta R(4 - jets)$ The smallest ΔR [4] between the four leading jets.

The first four leading jets and SumEt were selected as these parameters are used in the trigger definition. The $MIN\Delta R(4 - jets)$ corrects the angular distribution of the jets. This is important for triggers using the PacMan clustering algorithm which merges L2-clusters for jets which are close together.

One should note for this trigger study that only the shapes of the MC and data need to match. The absolute normalisation does not affect the measurement of trigger turn-on. In the analysis, the *Reweigh Matrix* and its numerator and denominator are implemented as a six-dimensional histogram. As the shape is only of concern, the six-dimensional histograms are normalised to unit area before the ratio is taken.

The application of this matrix is shown in equation 2. The MC event picks up a weight from the *Reweigh Matrix* and thus the distribution observed in data is reproduced.

$$\begin{aligned} &\text{Reweighed MC}[Jet1 - Et][Jet2 - Et][Jet3 - Et][Jet4 - Et][Sum - Et][MIN\Delta R(4 - jets)] \\ &= \text{MC}[Jet1 - Et][Jet2 - Et][Jet3 - Et][Jet4 - Et][Sum - Et][MIN\Delta R(4 - jets)] \\ &\times \text{Reweigh Matrix}[Jet1 - Et][Jet2 - Et][Jet3 - Et][Jet4 - Et][Sum - Et][MIN\Delta R(4 - jets)] \end{aligned} \quad (2)$$

Figure 3 gives an example of a derived *Reweigh Matrix* . The figure shows the numerator and denominator of the *Reweigh Matrix* . As a *sanity check*, one can remeasure the *Reweigh Matrix* after the *Reweigh Matrix* has been applied the MC; by definition all the elements should be 1. This is validated by the bottom-right plot of figure 3.

[4] $\Delta R = \sqrt{\Delta\eta^2 + \Delta\phi^2}$

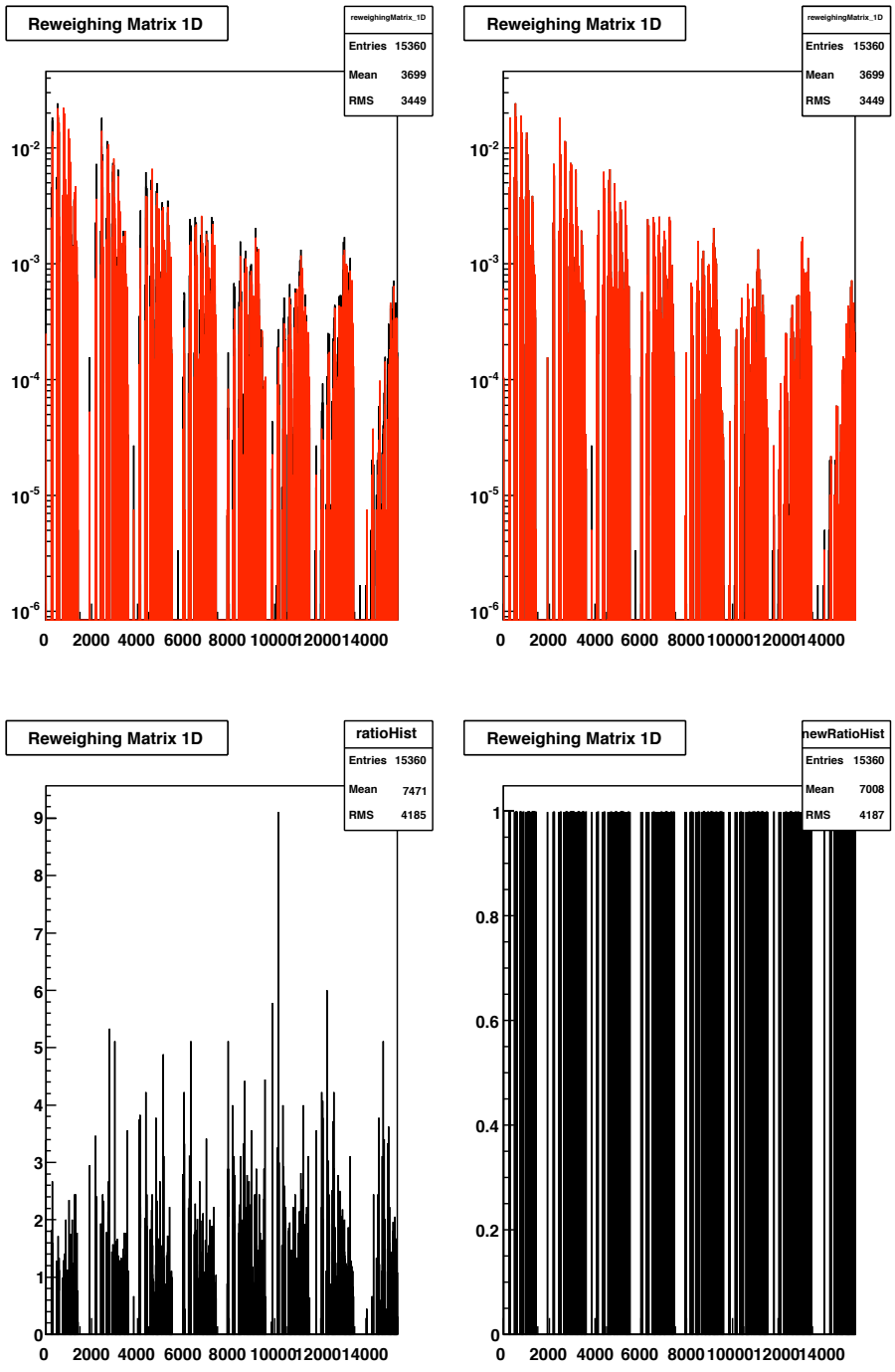

Figure 3: Example of *Reweigh Matrix* . The six-dimensional *Reweigh Matrix* is transformed into a one- dimensional vector. The x-axis for all of the histograms is the index of this transformed 1D vector. The top-left histogram are the MC (RED) and Data (BLACK) values. The ratio (thus the *Reweigh Matrix*) is shown in the bottom-left plot. The top-right plot is a copy of the top-left plot but after the *Reweigh Matrix* has been applied to the MC. As the *Reweigh Matrix* has been applied, the ratio of Data to MC should be 1 which is shown in the bottom- right plot.

5 Online Energy Correction

The previous trigger analysis note [2] showed rescaling the L2 cluster energies would help to match the MC & Data trigger turn-ons. In this note, the L2-cluster rescaling is derived from matching individual jets to individual L2 clusters rather than the global event variables like SumEt. Figure 4 (top-plots) show scatter plots of L2-Cluster Et matched to offline jets. A cluster is defined to match an offline jet by satisfying two requirements:

1. ΔR between the jet and L2-Cluster $<$ 0.3.
2. The minimum ΔR between jets $>$1.2. This jet isolation cut avoids merged clusters.

The scatter plots are converted into profile histograms (bottom-left plot of figure 4). The profile histograms show the L2-Cluster-Et scales linearly with Jet-Et but the MC matches to a higher energy L2 cluster compared to data. The consequence is that the MC would pass trigger cuts more often than data. Hence the MC trigger would turn-on before data. In order to correct for this difference, one should scale the MC L2 clusters to match the data L2 clusters. A bin-by-bin division of the profile histogram is shown in the bottom-right plot of figure 4. This ratio is does not vary with Jet-Et and so the points are fitted to a flat line; this ratio is the ONLINE ENERGY SCALE . It shows MC L2-Cluster Et need to be scale down by the ONLINE ENERGY SCALE of 0.93.

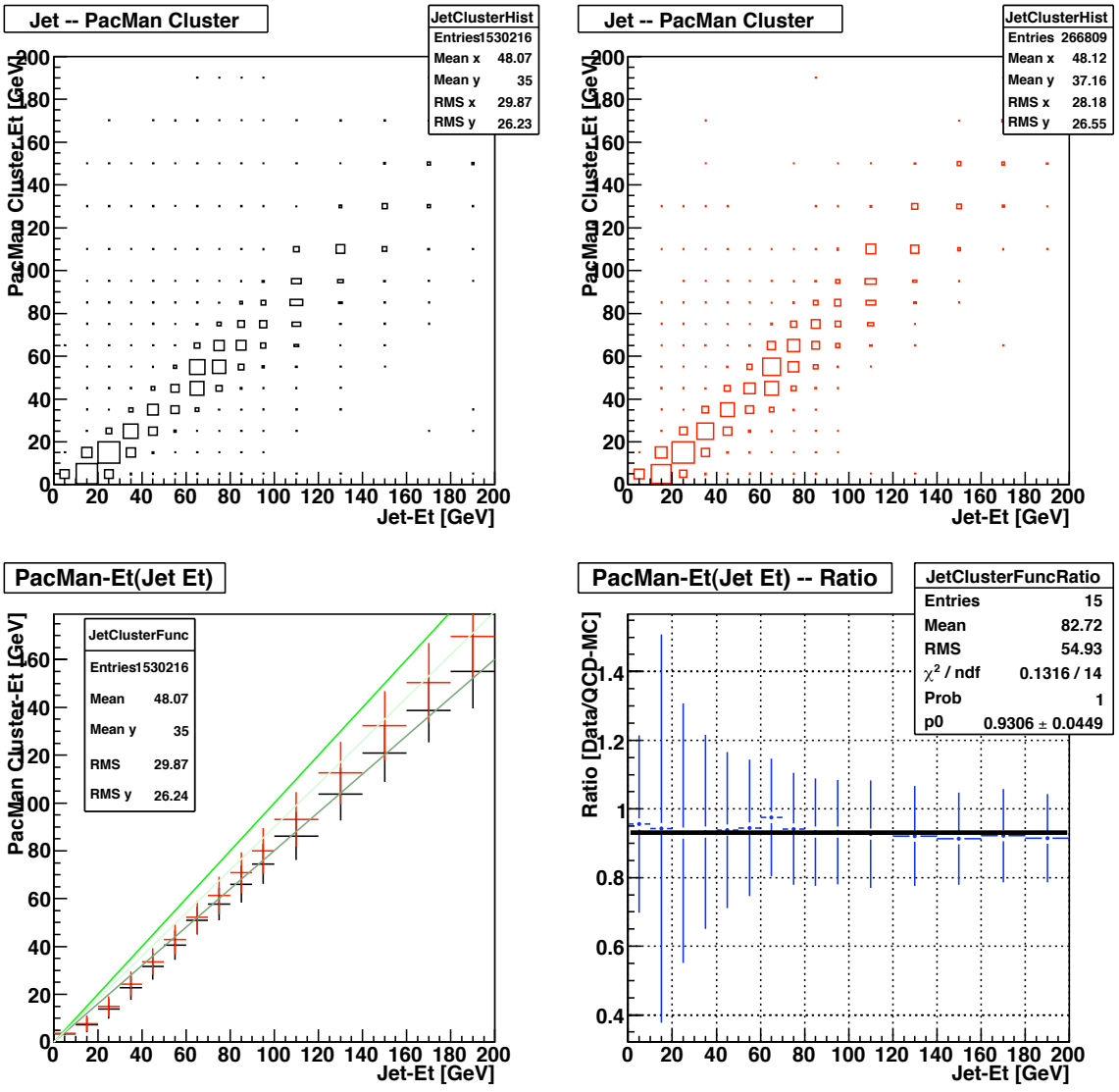

Figure 4: The top-left scatter plot shows the variation of L2-Cluster Et matched to offline jets for JET_50 data. The top-right plot is the equivalent plot for QCD-MC Pt40. The bottom-right are profile histograms of the scatter plots. The RED points are from QCD-MC P40 and the BLACK points are from JET_50 data. The green lines are straight lines with gradients of 1.0, 0.9 and 0.8; shown here as guide for the eye. The QCD-MC points tend to lie on the 0.9 gradient line while the data lies on 0.8 gradient line. So for the same jet, the MC would tend to give a large L2 cluster Et compared to data. The bottom-right plot is the bin-by-bin ratio of DATA/MC profile histograms. As the ratio is flat, it is fitted to a constant.

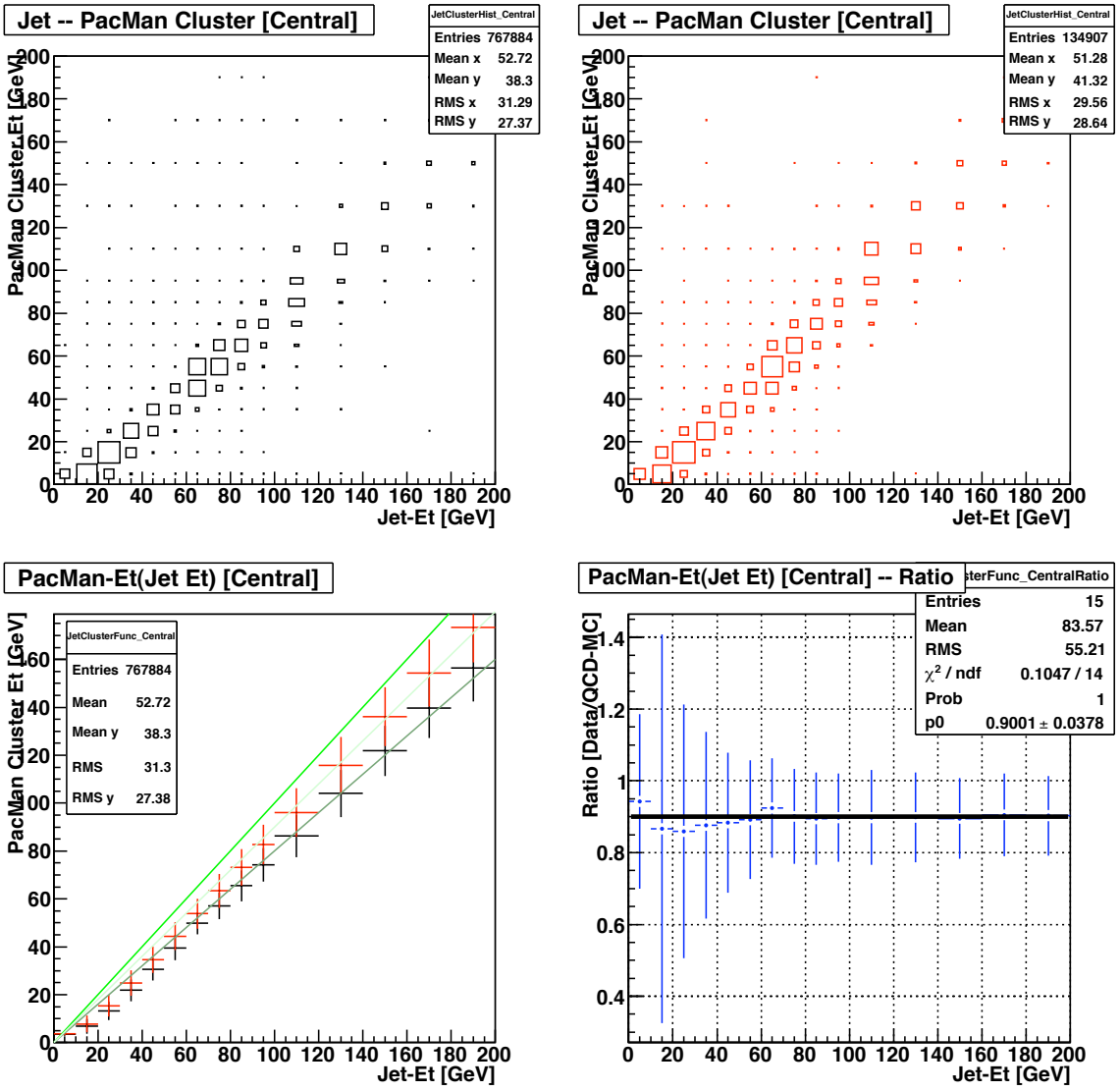

Figure 5: Derivation of ONLINE ENERGY SCALE for Central Calorimeter ($|\eta| < 1.1$). For the Central calorimeter, the ONLINE ENERGY SCALE scale is 0.9

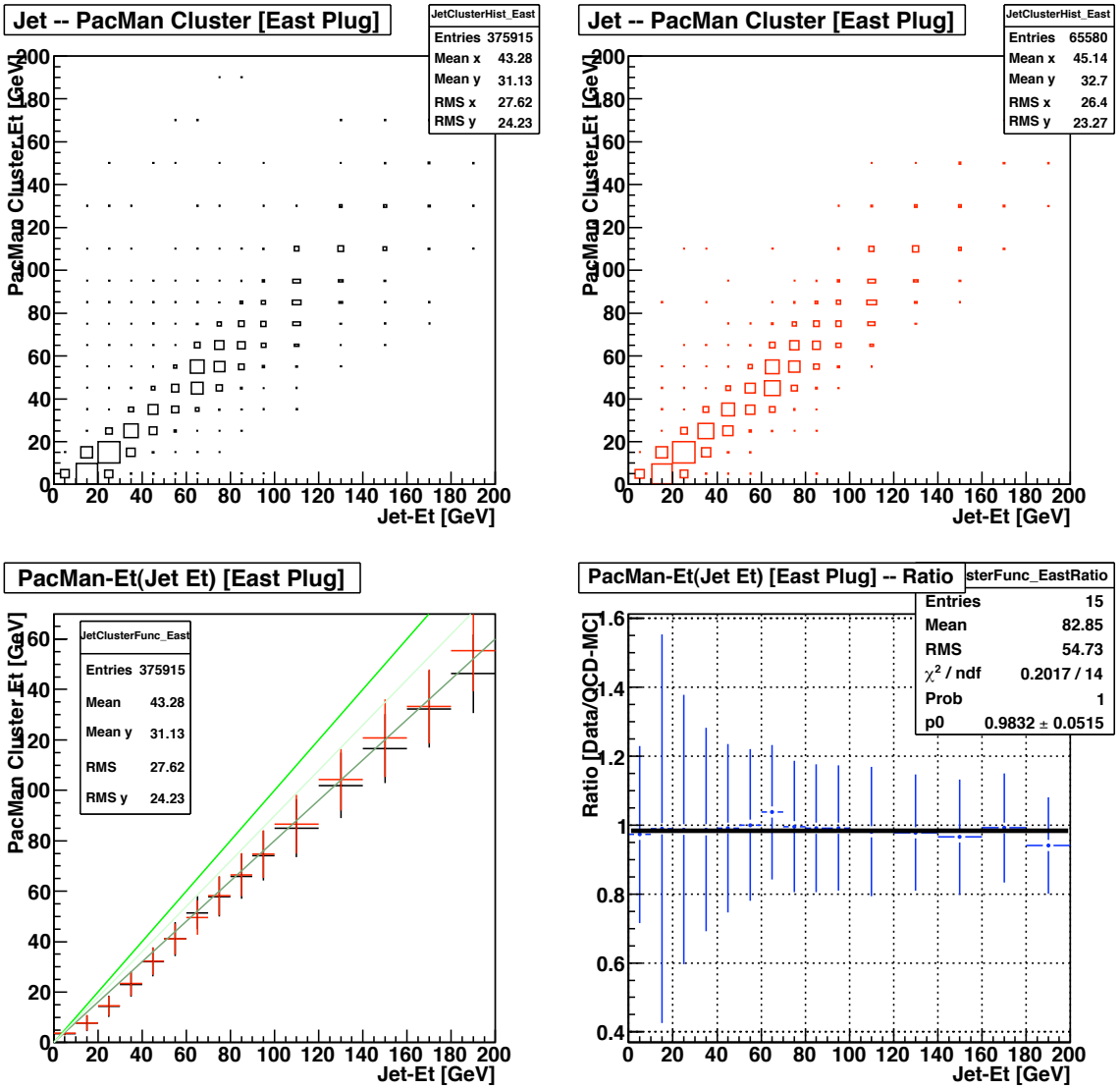

Figure 6: Derivation of ONLINE ENERGY SCALE for East Plug Calorimeter ($\eta > 1.1$). For the East Plug, the MC follows the DATA well. This is reflected in the ONLINE ENERGY SCALE of 0.98; very close to 1

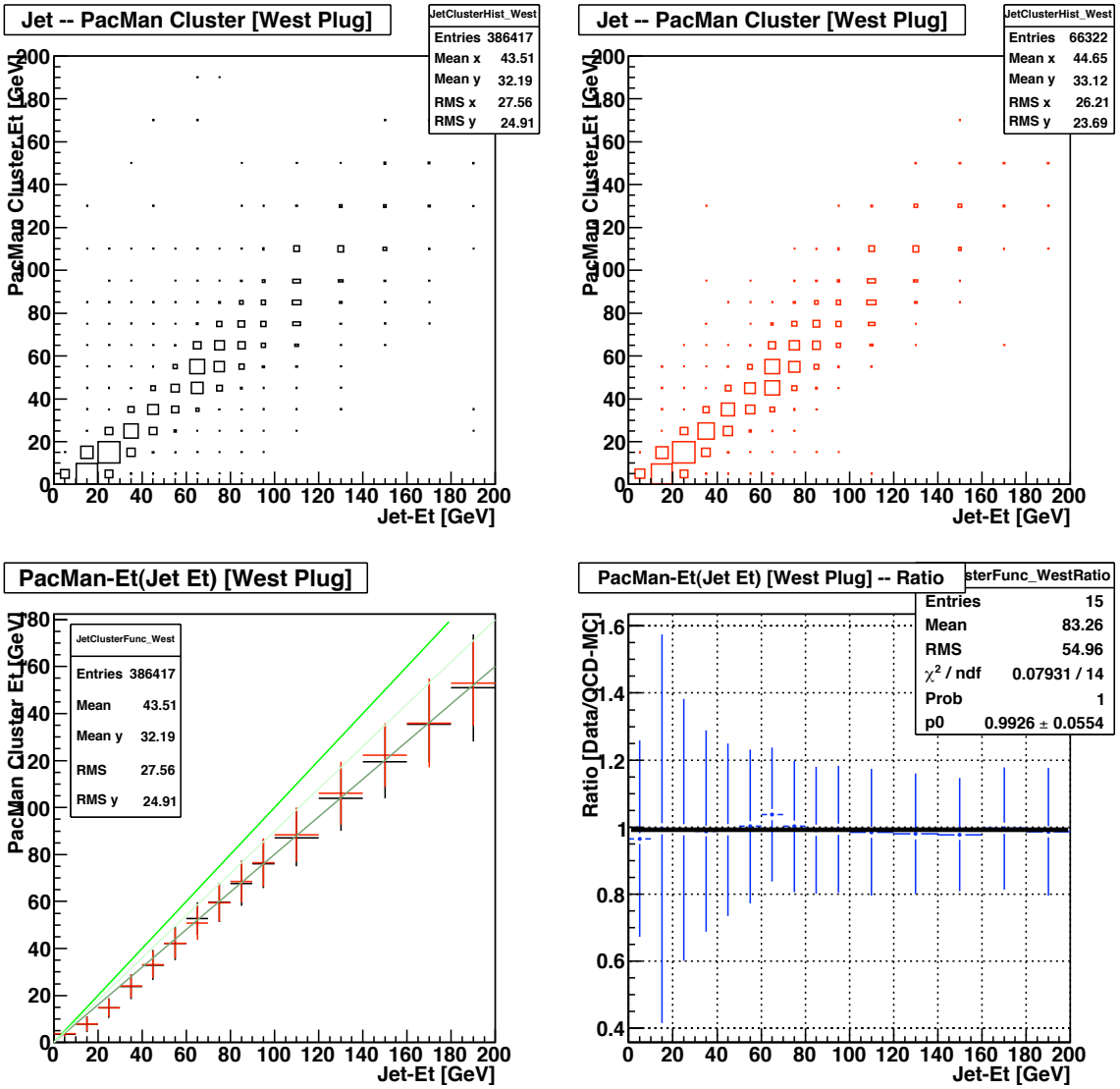

Figure 7: Derivation of ONLINE ENERGY SCALE for West Plug Calorimeter ($\eta < -1.1$). For the West Plug, the MC follows the DATA well. This is reflected in the ONLINE ENERGY SCALE of 0.99; basically 1

The previous trigger note [2] had shown this ONLINE ENERGY SCALE differs for the Plug and Central calorimeters. The ONLINE ENERGY SCALE was measured separately for East/West Plug and Central calorimeters (figures 5, 6, 7). The ONLINE ENERGY SCALE for East & West Plug calorimeters are approximately the same and the values are close to 1.0. So the MC models the Data well in the Plug regions. However for the central calorimeter, the ONLINE ENERGY SCALE is 0.9; a significant difference between the Data and MC L2 cluster scale.

Another dependence mentioned in the previous trigger study [2] was a Run-Number dependence. The ONLINE ENERGY SCALE was measured for different run-ranges and the variation is plotted in figure 8. As the run-number increases, the ONLINE ENERGY SCALE reduces. But when this is split by calorimeter type, the East & West Plug calorimeter have a constant ONLINE ENERGY SCALE . It is only the Central calorimeter which has a run-dependence. Figure 8 also shows the ONLINE ENERGY SCALE measured with WH Higgs MC sample. The ONLINE ENERGY SCALE has no sample dependence. The data from the plots are tabulated in table 1.

Table 1: Online Energy Scale: This table gives the scale to reduce the MC L2 cluster Et to make it match the response in data. The Central Calorimeter (CCAL) has a strong run dependence while the Plug Calorimeters (ECAL/WCAL) are independent of run number. So only the run-average (Full Run Range) value is used to correct the MC L2 Plug clusters. The break in the table are for the different L2 clustering algorithms. PACMAN was used from the start of Run-II to Run 246229 and L2-CONE started from Run 253134.

Run-Range	Whole	CCAL	ECAL	WCAL
138858 - 164386	0.955 ± 0.044	0.938 ± 0.038	1.062 ± 0.058	1.059 ± 0.056
164451 - 168640	0.930 ± 0.042	0.923 ± 0.038	0.945 ± 0.042	1.014 ± 0.037
168766 - 183783	0.946 ± 0.041	0.931 ± 0.036	0.988 ± 0.035	1.021 ± 0.052
183785 - 185517	0.933 ± 0.040	0.920 ± 0.036	1.010 ± 0.043	0.989 ± 0.046
185518 - 192504	0.938 ± 0.041	0.919 ± 0.037	0.923 ± 0.039	1.010 ± 0.050
192505 - 198686	0.923 ± 0.040	0.909 ± 0.035	0.984 ± 0.046	1.005 ± 0.050
198695 - 204640	0.928 ± 0.043	0.905 ± 0.037	1.026 ± 0.051	1.010 ± 0.052
204642 - 211265	0.913 ± 0.041	0.892 ± 0.036	0.956 ± 0.043	1.007 ± 0.045
211267 - 222551	0.909 ± 0.043	0.888 ± 0.037	1.011 ± 0.052	1.005 ± 0.055
222552 - 232781	0.889 ± 0.041	0.868 ± 0.036	0.991 ± 0.051	1.020 ± 0.046
232802 - 239906	0.895 ± 0.042	0.872 ± 0.036	1.002 ± 0.042	1.077 ± 0.042
239923 - 246229	0.880 ± 0.041	0.857 ± 0.034	0.944 ± 0.050	1.011 ± 0.060
Full Run Range	0.919 ± 0.043	0.902 ± 0.038	1.001 ± 0.052	1.008 ± 0.054
253134 - 255940	0.891 ± 0.051	0.858 ± 0.047	0.890 ± 0.033	1.011 ± 0.061
255941 - 257698	0.874 ± 0.050	0.849 ± 0.046	0.980 ± 0.048	0.993 ± 0.054
257706 - 259590	0.871 ± 0.053	0.843 ± 0.049	0.976 ± 0.061	0.972 ± 0.056
259591 - 261143	0.872 ± 0.052	0.844 ± 0.046	0.973 ± 0.062	0.988 ± 0.061
Full Run Range	0.875 ± 0.052	0.844 ± 0.047	0.987 ± 0.060	0.995 ± 0.061

The run dependence of the ONLINE ENERGY SCALE for the Central Calorimeter could be attributed to the detector response changing with time (Run-Number). The profile histograms show the L2 Cluster Et Vs Jet-Et can be fitted to a straight line. The variation in offset and

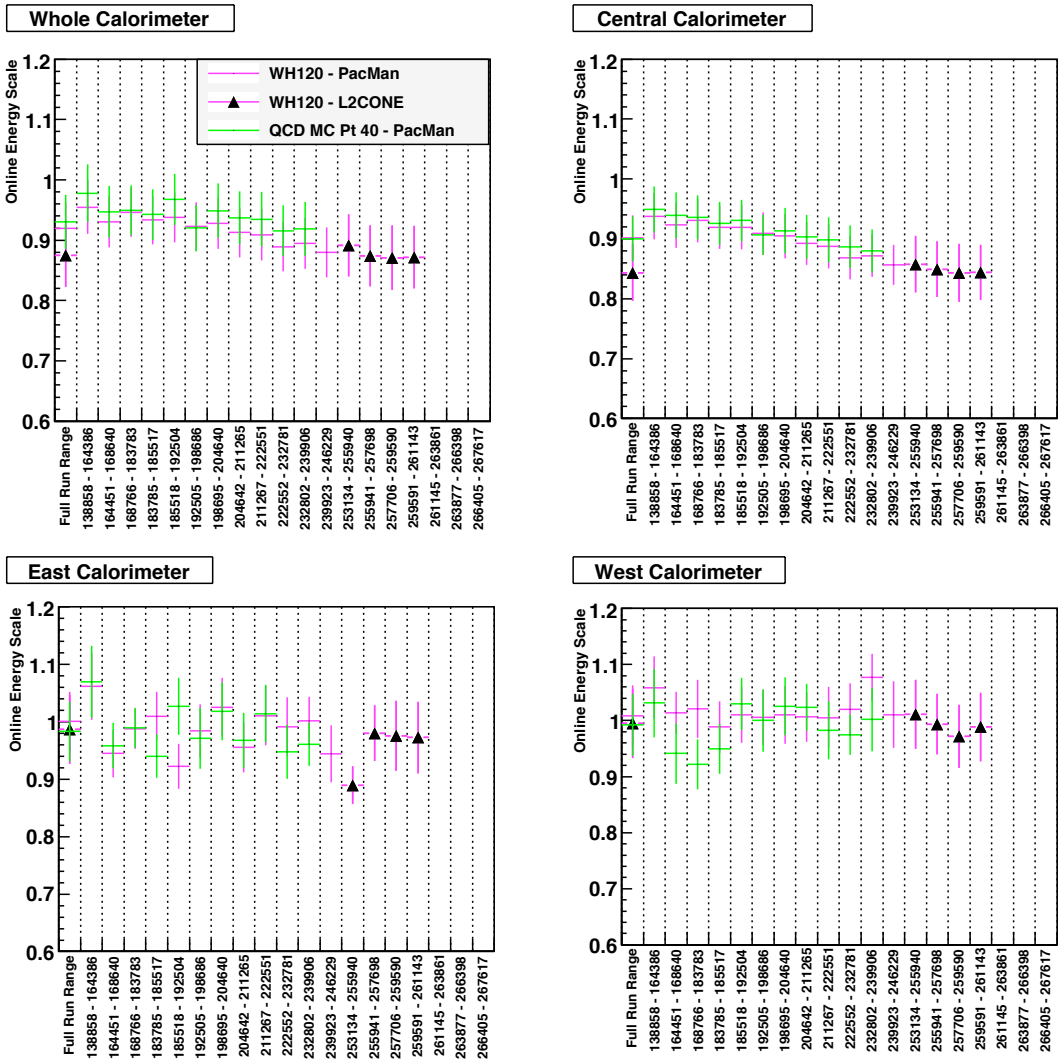

Figure 8: Run Dependent ONLINE ENERGY SCALE . Each plot shows the variation of the ONLINE ENERGY SCALE as a function of Run-Number for Whole Calorimeter (top-left), Central Calorimeter (top-right), East Plug (bottom-left) and West Plug (bottom-right). The observed run dependence is only for the Central calorimeter while the Plug does not vary. The plots also show the ONLINE ENERGY SCALE does not depend on the MC sample as both QCD-MC Pt 40 and WH-MC give the same values.

slope for each run period is shown in figures 9 & 10. The offset does not vary except when the L2 clustering algorithm is changed. However the slope for the MC changes with run number, but only when the PacMan clustering algorithm is used. The slope for data does not vary with run number except a step when the L2 clustering algorithm was changed. This shows the run dependence of the Central Calorimeter ONLINE ENERGY SCALE is to compensate for the the MC L2 cluster energy changing with time/Run-Number. Further investigation into this run dependency was shown to be due to a bug in CDF-code [5].

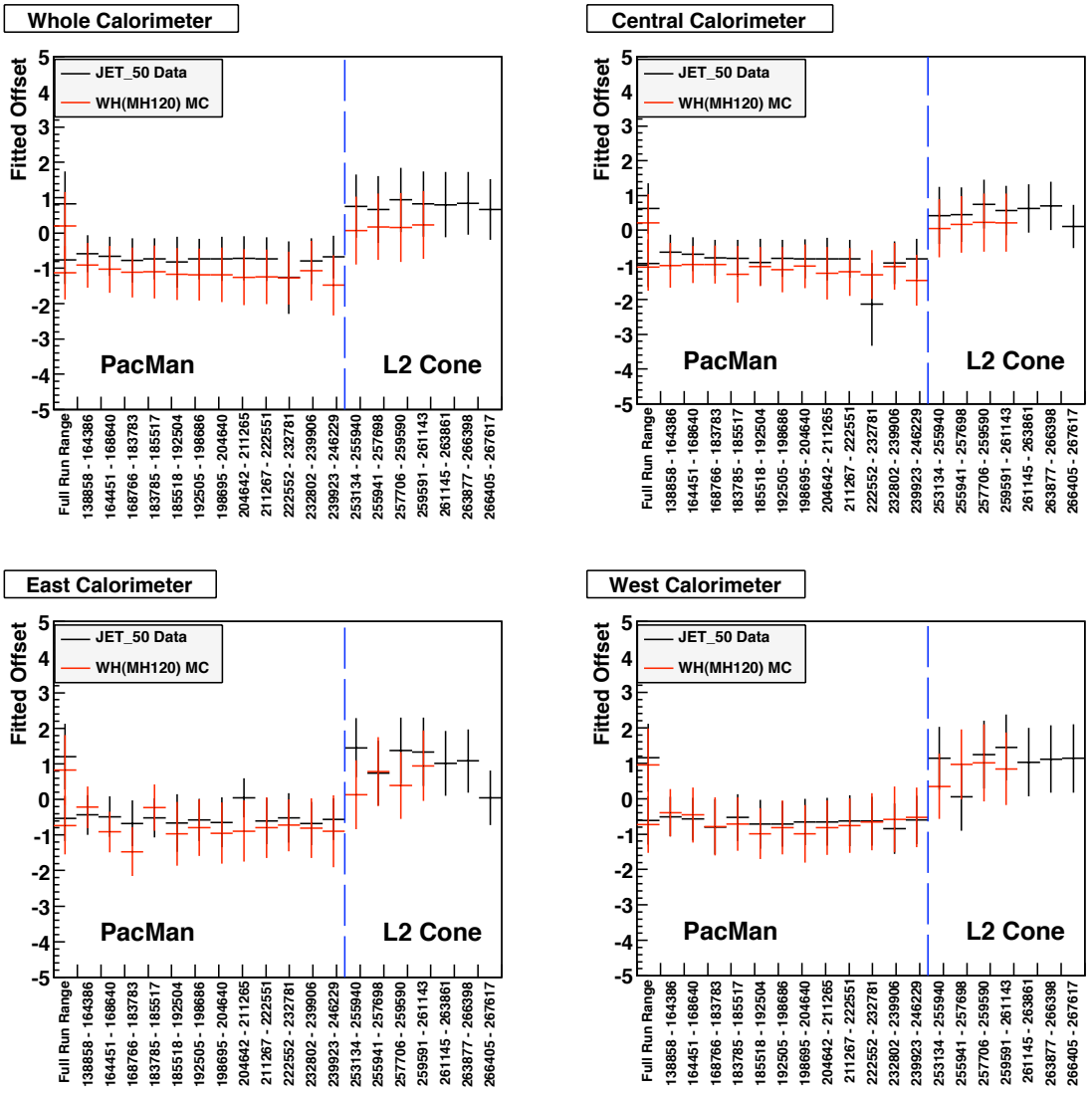

Figure 9: The L2-Cluster Et Vs Jet-Et profile histograms are fitted to straight lines. The graphs show the variation of the fitted offset with run number for the whole, central, East & West calorimeter. The offset only changes when the L2 clustering algorithm changes.

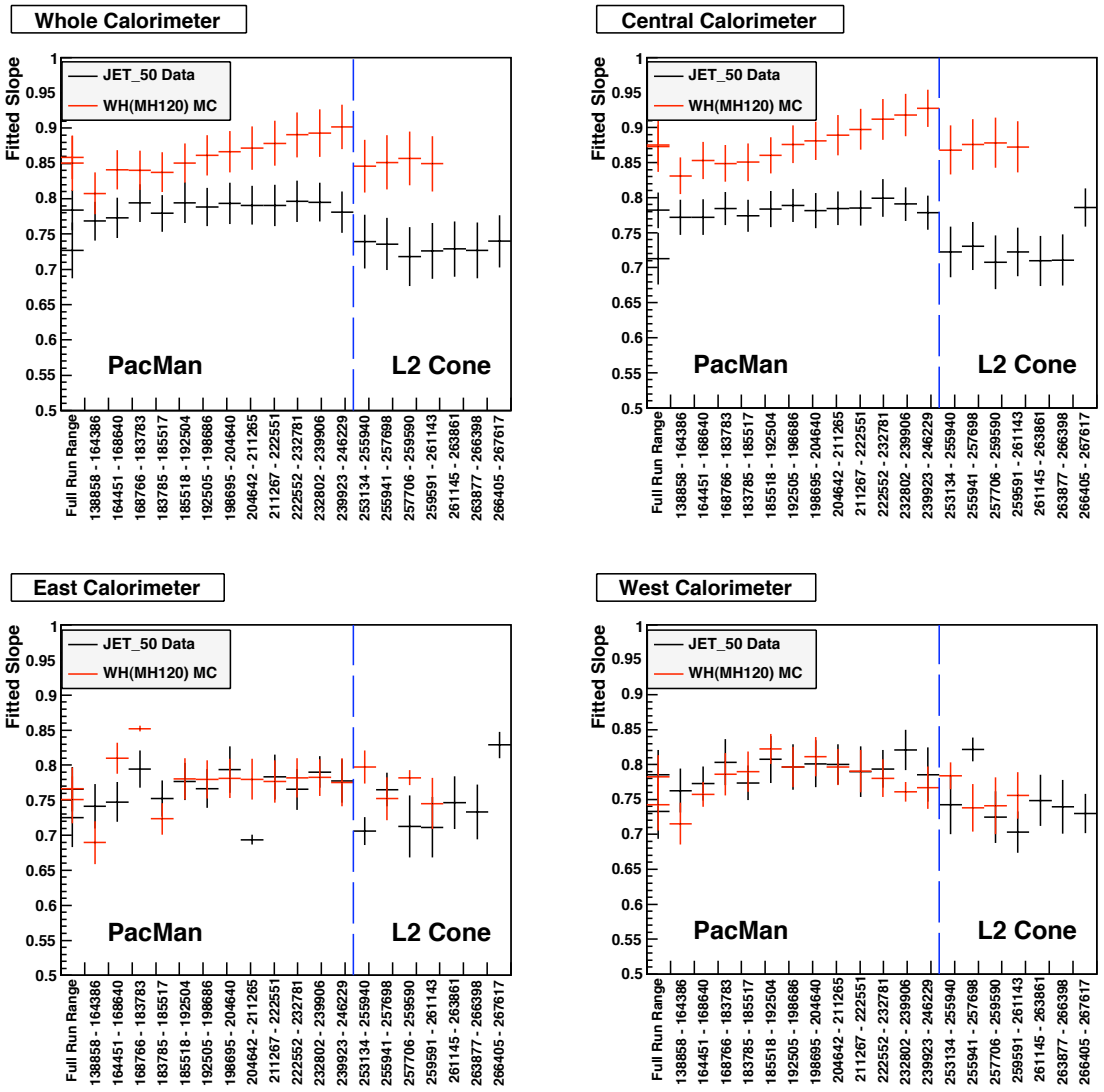

Figure 10: The L2-Cluster Et Vs Jet-Et profile histograms are fitted to straight lines. The graphs show the variation of the fitted gradient (slope) with run-number for Whole, Central, East & West calorimeter. The MC (Red) and data (Black) fitted slopes for the Plug calorimeters agree with each other. However the slopes for the central calorimeter are do not agree. The data does not vary with run number except when the L2 clustering algorithm changed. But the MC shows a continuous increase in the slope until the L2 clustering algorithm changed. So the run dependency of the online energy scale is to compensate for the MC change in gradient.

6 TOP_MULTI_JET **Trigger**

The signature for VH/VBF all-hadronic mode are 4 high-P_T jets with large Sum-Et. The TOP_MULTI_JET trigger was designed to trigger on such events. There have been 12 versions of this trigger during Run-II. However they can be categorised into 4 major versions.

- L1_JET10_ &_SUMET130 and L2_AUTO_L1_JET10_&_SUMET130 (V2)
- L1_JET10 and L2_FOUR_JET125_SUMET(V3-V4)
- L1_JET10 and L2_FOUR_JET175_SUMETV5-V8)
- L1_JET20 and L2_FOUR_JET175_SUMET(V9)
- Same trigger definition as V9 but L2-Cone clustering is used (V12)

The trigger versions not mentioned in the list are not associated with any Good-Runs. For simplicity, TOP_MULTI_JET_V2-V4 are remade using the V8 definition; i.e. the L2 SumEt cut is raised from 125 GeV to 175ĠeV.

Table 2 shows the number of L1, L2 & L3 triggers fired for each version of TOP_MULTI_JET. The table shows the L2 component has the tightest cuts. So the focus is on matching the L2 performance.

Table 2: Rate for L1, L2 & L3 firing for TOP_MULTI_JET. The table shows the number of times L1, L2 and L3 triggers fired for the high-P_T Muon dataset after passing the standard event selection. The L1 Rate is defined as (L1 && L2/L2) and the L3 Rate is defined as (L1 && L2 && L3 / L1 && L2). The L3 rate shows the L3 trigger will always fire if the event has passed L1 and L2. The L2 rate shows L1 trigger would have fired if the L2 trigger had fired. The exceptions are the last two versions of TOP_MULTI_JET where the L1 trigger was raised from L1_JET10 to L1_JET20. This caused a 4% loss and will need to be accounted for.

TOP_MULTIJET Version	L1 Count	L2 Count	(L1 && L2) Count	(L1 && L2 && L3) Count	L1 Rate	L3 Rate
TOP_MULTIJET v-1	0	0	0	0	0	0
TOP_MULTIJET v-2	0	0	0	0	0	0
TOP_MULTIJET v-3	16848	2155	2155	2142	1	0.994
TOP_MULTIJET v-4	99979	14629	14560	14427	0.995	0.991
TOP_MULTIJET v-5	17071	1359	1347	1335	0.991	0.991
TOP_MULTIJET v-6	35518	2497	2495	2487	0.999	0.997
TOP_MULTIJET v-7	0	0	0	0	0	0
TOP_MULTIJET v-8	90513	6566	6562	6541	0.999	0.997
TOP_MULTIJET v-9	607248	80679	77055	76728	0.955	0.996
TOP_MULTIJET v-10	0	0	0	0	0	0
TOP_MULTIJET v-11	0	0	0	0	0	0
TOP_MULTIJET v-12	1306835	273665	262762	260312	0.960	0.991
All Versions	2174012	381550	366936	363972	0.962	0.992

6.1 TOP_MULTI_JET_**V2-V8**

The TOP_MULTI_JET trigger for V2-8 is defined as:

Level 1 L1_JET10

Level 2 L2_FOUR_JET15_SUMET175

Level 3 Four 15 GeV 0.4 cone jets

As mentioned in the previous section, the Level-2 SumEt cut has been set to 175 GeV for V2-V4 of TOP_MULTI_JET to simplify the analysis.

The first step for this analysis is to derive a *Reweigh Matrix* for QCD-MC such that the input distributions match those measured in data. Figure 11 shows the input distributions of the QCD-MC before and after the reweigh matrix has been applied. After the *Reweigh Matrix* has been applied, it matches the Data exactly. The two start to diverge in the tails where statistics are low.

After the *Reweigh Matrix* , one has to apply the ONLINE ENERGY SCALE to the Level-2 clusters to correct their energy. For this version of the TOP_MULTI_JET trigger, only the Level-2 trigger needs to be emulated. Figure 12 shows the application of the corrections upon the measured trigger turn-on. If the raw QCD-MC is used, the TOP_MULTI_JET trigger is over-efficient with respect to data.

After the corrections, the QCD-MC matches the data better. The bottom row of figure 12 shows the ratio of the trigger turn-ons of JET_50 data to QCD-MC (after correction). They are flat with ratios close to 1.0. The fitted ratio for the TOP_MULTI_JET trigger of the Data to the QCD-MC(corrected) is 0.963 ± 0.008. This ratio is applied as a scale factor to the MC trigger.

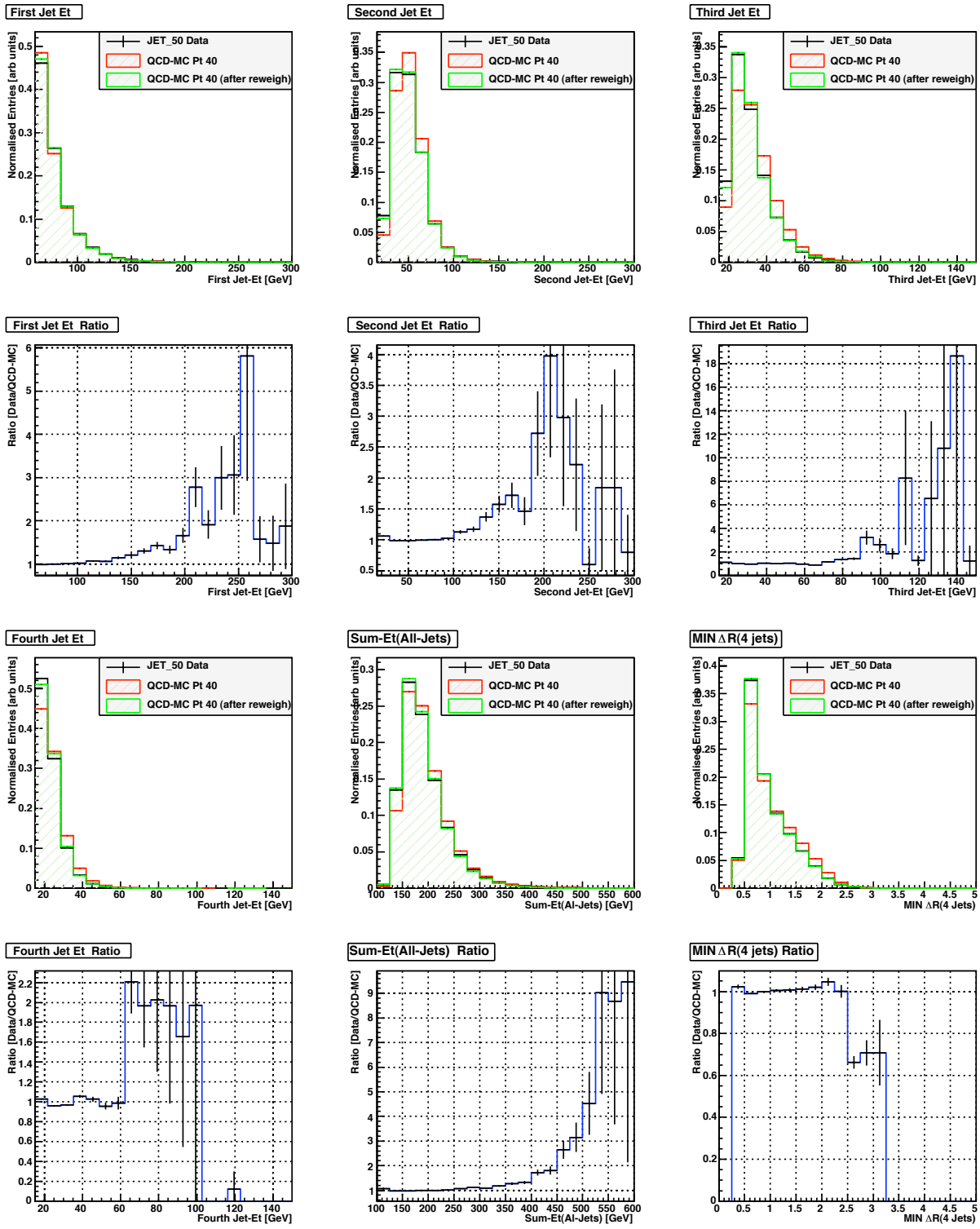

Figure 11: Jet, Sum-Et & MIN ΔR distributions: The reweigh matrix is applied to the QCD-MC Pt40 which makes the distributions match JET_50 data.

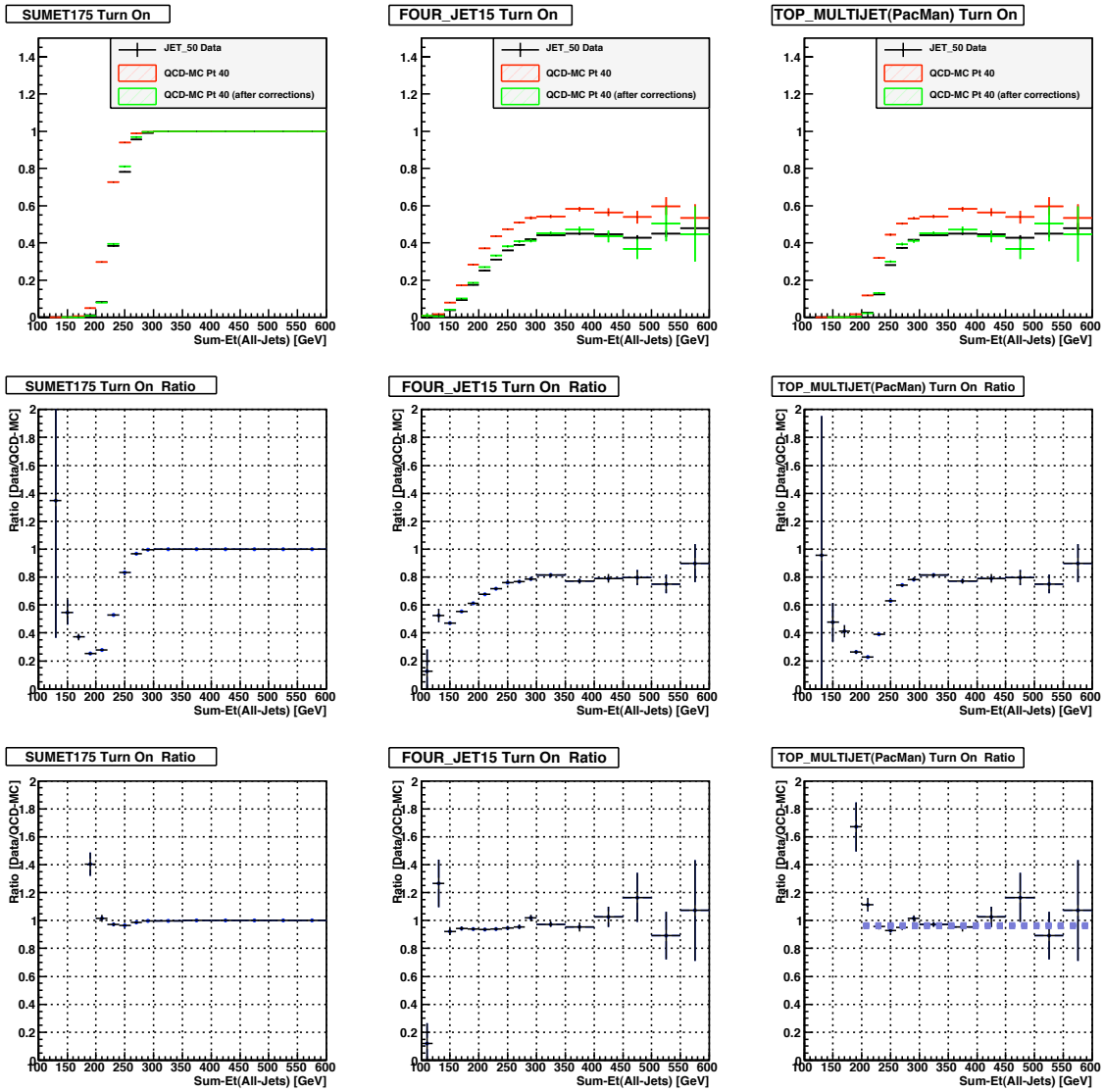

Figure 12: The trigger turn on for the L2 TOP_MULTI_JET components. The middle row shows ratio ratio of JET_50 data to QCD-MC(uncorrected). The bottom row shows the ratio of JET_50 data to QCD-MC(corrected). After the correction, the QCD-MC trigger turn-on agrees better the JET_50 data. The fitted ratio for the TOP_MULTI_JET trigger of the Data to the QCD-MC(corrected) is 0.963 ± 0.008

6.2 TOP_MULTI_JET_V9

During Period 7, the L1 jet trigger threshold was raised from 10 GeV to 20 GeV which reduced the acceptance by $\approx 6\%$. As we cannot assume L1 jet trigger would fire if L2 is true, the L1_JET20 trigger needs to be measured. Figure 13 shows the L1_JET20 turn on if Level-2 of TOP_MULTI_JET had fired. The turn-on measured by MC does not match the data. The ratio of the two turn-ons is shown in the adjacent plot and fitted to function in equation 3. This function is applied to events passing Level-2 TOP_MULTI_JET trigger.

$$f(x) = A\left(1 - \exp^{-Bx}\right) + C \tag{3}$$

x : Sum-Et(All-Jets)

After the fit, the parameters for the turn-on are:

A 19.23 ± 0.01

B 0.0280 ± 0.0004

C -18.24 ± 0.01

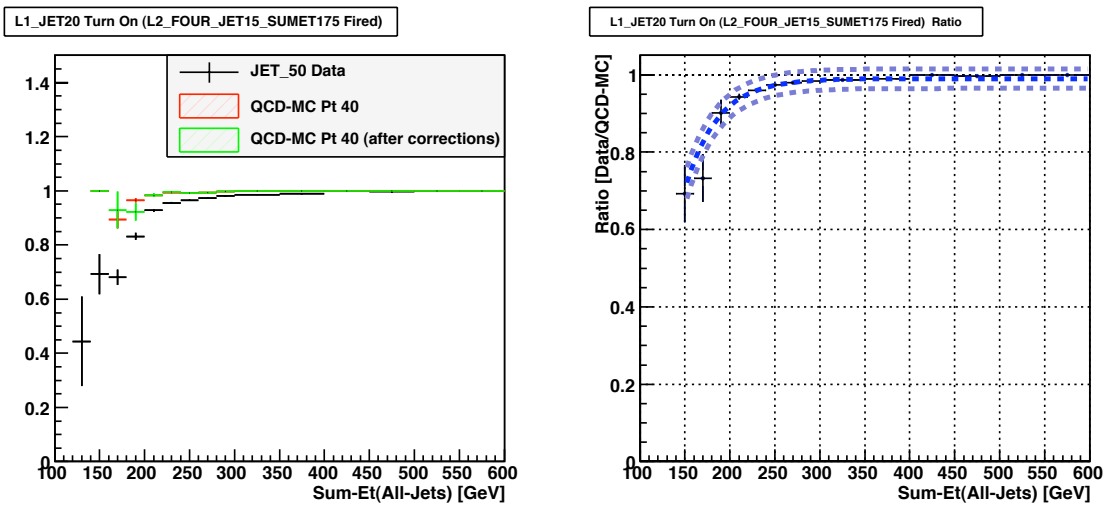

Figure 13: L1_JET20 correction: The left-graph shows the turn-on for L1_JET20 for events passing the standard event selection and the L2 trigger. The right-graph shows the ratio of the turn-on for data to the corrected QCD-MC. This ratio is fitted to equation 3 and plotted (dark blue line). The lighter blue lines are $\pm 1\sigma$ variation of the fit parameters.

Due to this L1_JET20 turn-on correction, the overall MC scale-factor is $0.963 \times f(x)$ (scale factor from section 6.1 and L1_JET20 turn on from equation 3).

6.3 TOP_MULTI_JET_**V12**

After the 2007 shutdown, the level-2 calorimeter trigger clustering was changed from PAC-MAN to L2-CONE . A major advantage of the L2-CONE algorithm is that is does not suffer from cluster merging which impaired the PACMAN algorithm. Further details can be found in [3]. Another improvement after the shutdown was the Tevatron performance. There were substantial gains in the instantaneous & integrated luminosity (see figure 14). Unfortunately the available QCD-MC samples only go to P11. They do not include the L2-CONE clusters or reflect the post 2007 shutdown luminosity profile. This was corrected by:

- Adding Number-of-Verticies (NVertex) to the *Reweigh Matrix*
- Remake all the L2 clusters using L2-CONE

The *Reweigh Matrix* is now a seven dimensional histogram to ensure the QCD-MC has the correct luminosity profile (see equation 4).

$$\text{Reweigh Matrix}[Jet1-Et][Jet2-Et][Jet3-Et][Jet4-Et][Sum-Et][MIN\Delta R(4-jets)][N-Vertex] = \frac{\text{Data}[Jet1-Et][Jet2-Et][Jet3-Et][Jet4-Et][Sum-Et][MIN\Delta R(4-jets)][N-Vertex]}{\text{MC}[Jet1-Et][Jet2-Et][Jet3-Et][Jet4-Et][Sum-Et][MIN\Delta R(4-jets)][N-Vertex]} \quad (4)$$

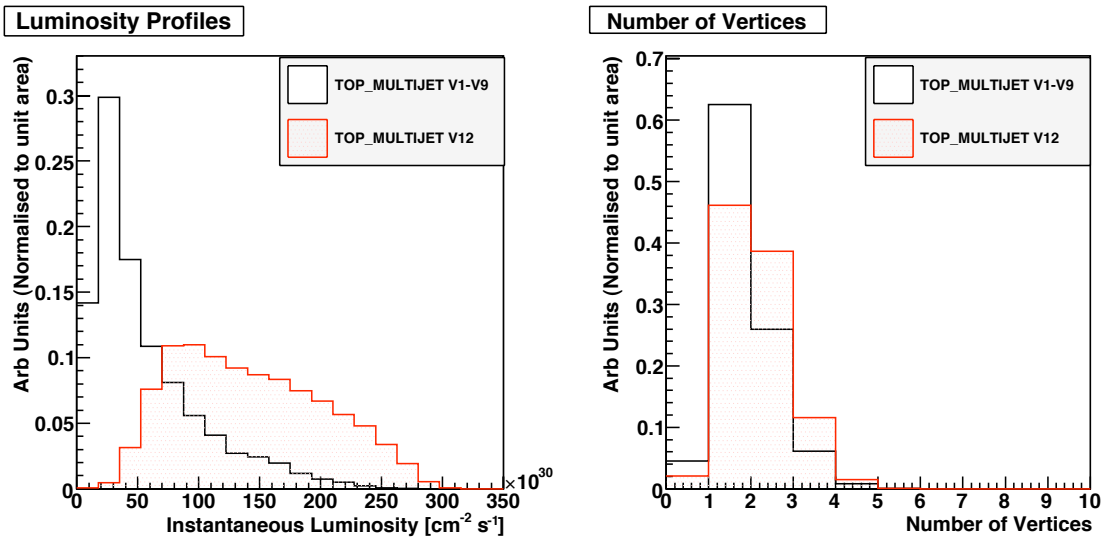

Figure 14: Changes is luminosity profile: After the 2007 shutdown, the Tevatron luminosity profile changed substantially. The graph on the left shows the instantaneous lumi profile for JET_50 data for TOP_MULTI_JET_V1-9 and TOP_MULTI_JET_V12. The instantaneous luminosity before and after are quite different. The plot on the right shows the number of vertices for the two periods. Again the graphs shows JET_50 data normalised to unit area. The higher instantaneous luminosity gives rise to more vertices being recorded.

Figure 15 shows the Data and QCD-MC distributions before/after the Seven-Dimensional *Reweigh Matrix* is applied. After the correction, the QCD-MC now has the same luminosity profile (N-Vertex distribution).

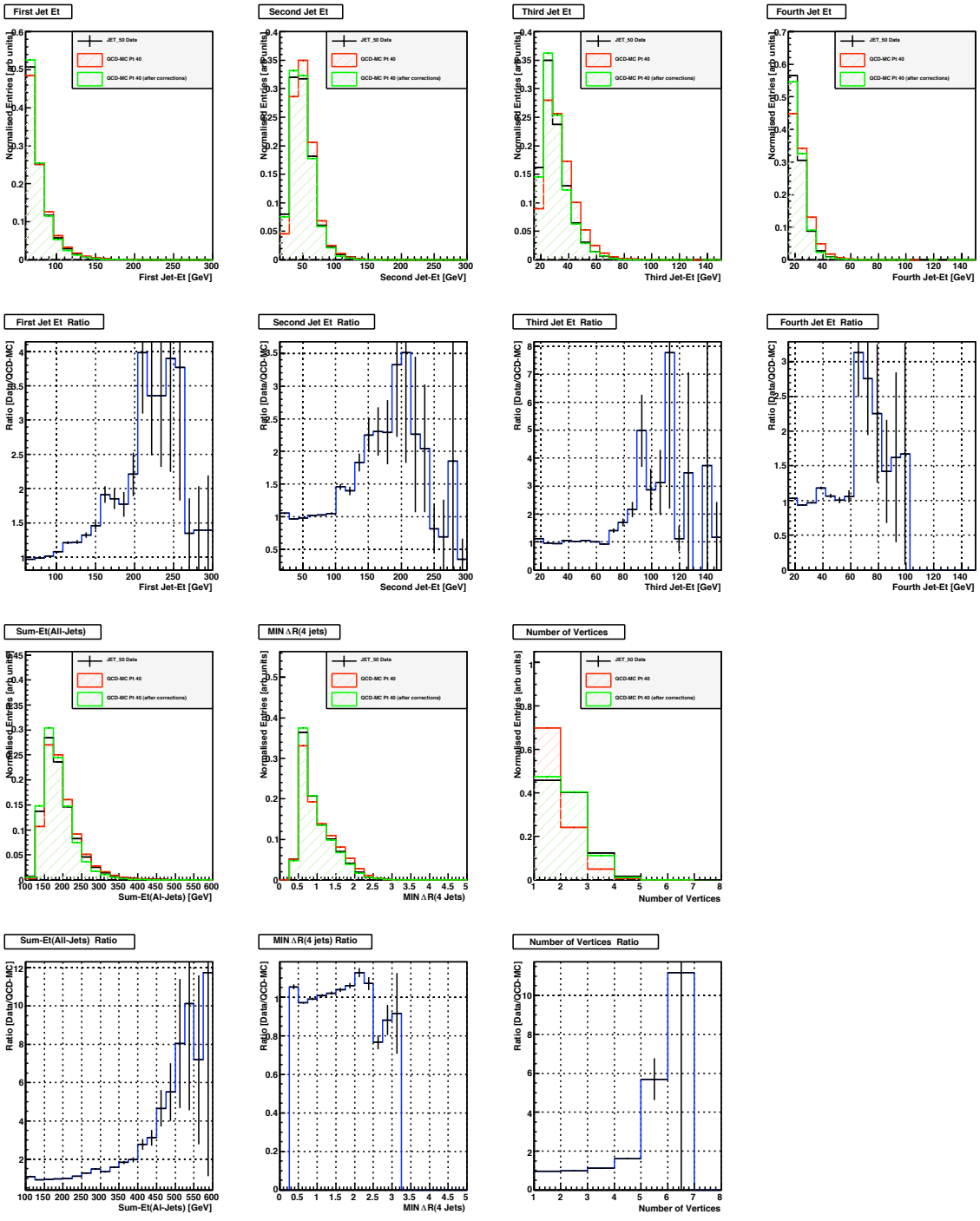

Figure 15: The Jet-Et, Sum-Et, MIN ΔR & N-Vertex distribution. For the L2-CONE data, the luminosity profile changed in data changed substantially. So in addition to the event kinematics, the N-Vertex distribution is reweighed. After the reweigh matrix is applied, the QCD-MC follows the data.

As the run-ranges for QCD-MC and the JET_50 data do not overlap, the ONLINE ENERGY SCALE needs to be considered. Section 5 had shown only the MC had a run-dependency. To check the ONLINE ENERGY SCALE of this disjoint data, the ONLINE ENERGY SCALE was remeasured but:

- QCD-MC ran over all of its events but all L2-Cluster remade using L2-CONE
- The JET_50 data was restricted to TOP_MULTI_JET_V-12

The QCD-MC was split into the same run sections as defined in table 1. But all of the analysed JET_50 data was examined as we know there is no run dependency in data. The result of this ONLINE ENERGY SCALE is shown in table 3. The values are same as those using PacMan. So one can use the same ONLINE ENERGY SCALE .

The same procedure as in section 6.1 was followed to correct the QCD-MC Pt40: the QCD-MC was reweighed using the reweigh matrix defined in equation 4 and the L2-CONE clusters were rescaled using the values in table 1. Figure 16 shows the TOP_MULTI_JET_V-12 trigger turn-ons for JET_50 data and QCD-MC Pt40 before and after the corrections are applied. The bottom row of figure 16 are the ratios of the trigger turn-ons of JET_50 data to the corrected QCD-MC Pt40. The fitted ratio for TOP_MULTI_JET is 0.973 $\pm$ 0.006.

The L1 trigger for TOP_MULTI_JET_V-12 is L1_JET20. Figure 17 shows the turn-on for L1_JET20 for events passing the standard event selection and L2 components of TOP_MULTI_JET_V-12. The ratio of JET_50 to corrected QCD-MC for the L1_JET20 turn-on is fitted to equation 5.

$$f(x) = A\left(1 - \exp^{-Bx}\right) \tag{5}$$

x : Sum-Et(All-Jets)

After the fit, the parameters for the turn-on are:

A 0.994 ± 0.001

B 0.0132 ± 0.0003

The overall MC scale factor for TOP_MULTI_JET_V-12 is $0.973 \times f(x)$ (as defined in equation 5).

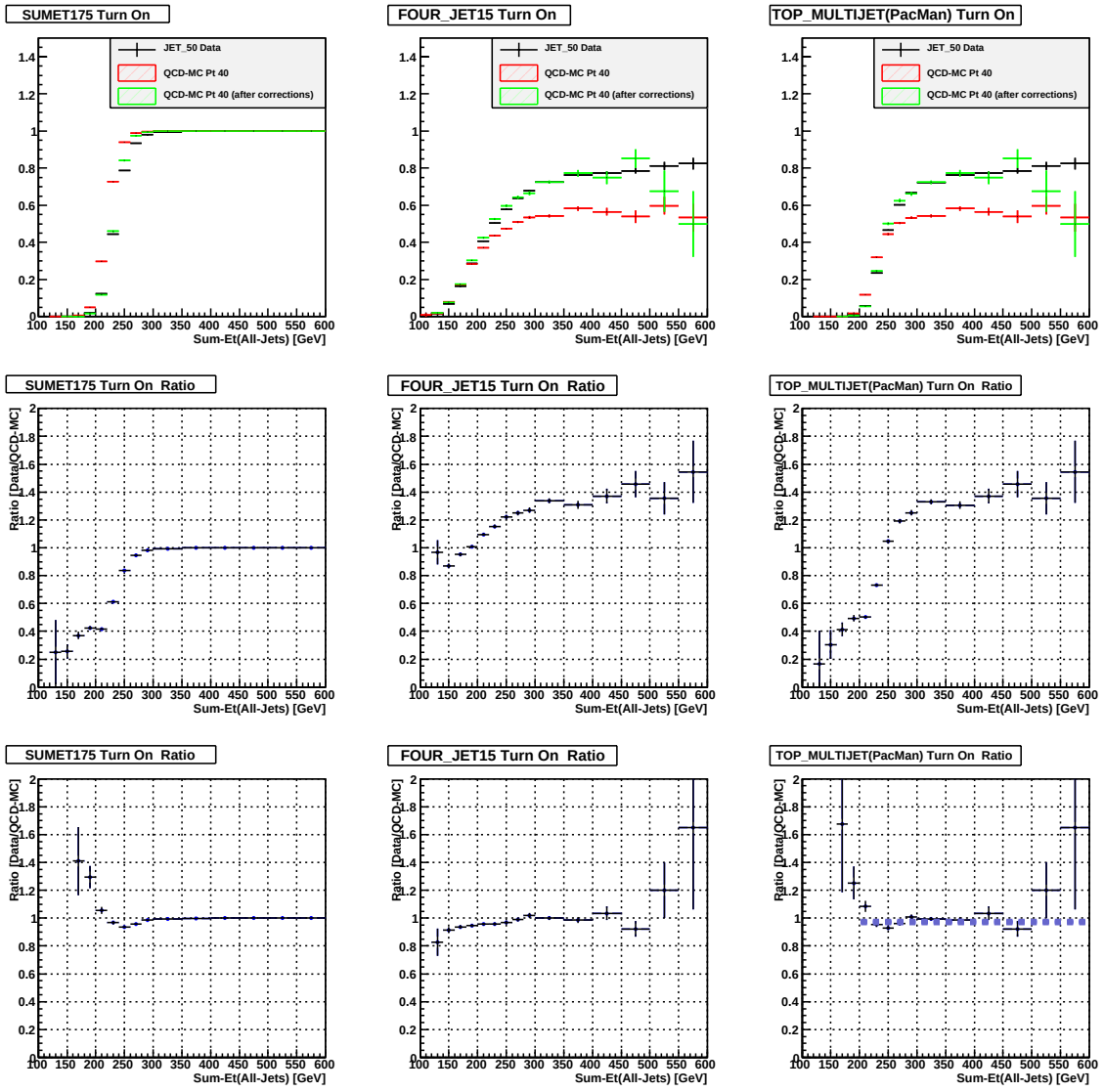

Figure 16: The Trigger Turn On for TOP_MULTI_JET_V-12 : The top row shows the L2 trigger trigger turn on for TOP_MULTI_JET and its components. The middle row shows the ratio of JET_50 data to QCD-MC(uncorrected). The bottom row shows the ratio of JET_50 data to QCD-MC(corrected). The fitted ratio for TOP_MULTI_JET_V-12 is 0.973 ± 0.006.

Table 3: Online Energy Scale: The QCD-MC only goes to P11 which does not cover the L2-CONE period. As the MC has run-depdendcy on the L2-Cluster Et, one needs to cross-check the ONLINE ENERGY SCALE . The ONLINE ENERGY SCALE was remeasured using the all (good) runs from QCD-MC but the clusters are remade using the L2-CONE algorithm. The data was restricted to the L2-CONE period (TOP_MULTI_JET_V12). The measured energy scale is the same.

Run-Range	Whole	CCAL	ECAL	WCAL
138858 - 164386	0.988 ± 0.058	0.944 ± 0.049	1.116 ± 0.075	1.067 ± 0.071
164451 - 168640	0.944 ± 0.052	0.927 ± 0.048	0.991 ± 0.058	0.957 ± 0.062
168766 - 183783	0.931 ± 0.052	0.914 ± 0.048	0.975 ± 0.057	0.929 ± 0.057
183785 - 185517	0.937 ± 0.053	0.916 ± 0.048	0.991 ± 0.057	0.955 ± 0.059
185518 - 192504	0.938 ± 0.052	0.905 ± 0.046	1.005 ± 0.062	0.985 ± 0.051
192505 - 198686	0.907 ± 0.050	0.887 ± 0.046	0.989 ± 0.063	0.988 ± 0.064
198695 - 204640	0.921 ± 0.052	0.888 ± 0.047	0.992 ± 0.059	0.986 ± 0.054
204642 - 211265	0.917 ± 0.053	0.881 ± 0.047	0.983 ± 0.059	0.979 ± 0.053
211267 - 222551	0.914 ± 0.053	0.874 ± 0.046	0.994 ± 0.059	0.949 ± 0.054
222552 - 232781	0.902 ± 0.051	0.866 ± 0.046	0.966 ± 0.058	0.961 ± 0.053
232802 - 239906	0.898 ± 0.053	0.855 ± 0.046	0.977 ± 0.058	0.976 ± 0.060
Full Run Range	0.918 ± 0.053	0.882 ± 0.047	0.992 ± 0.060	0.975 ± 0.059

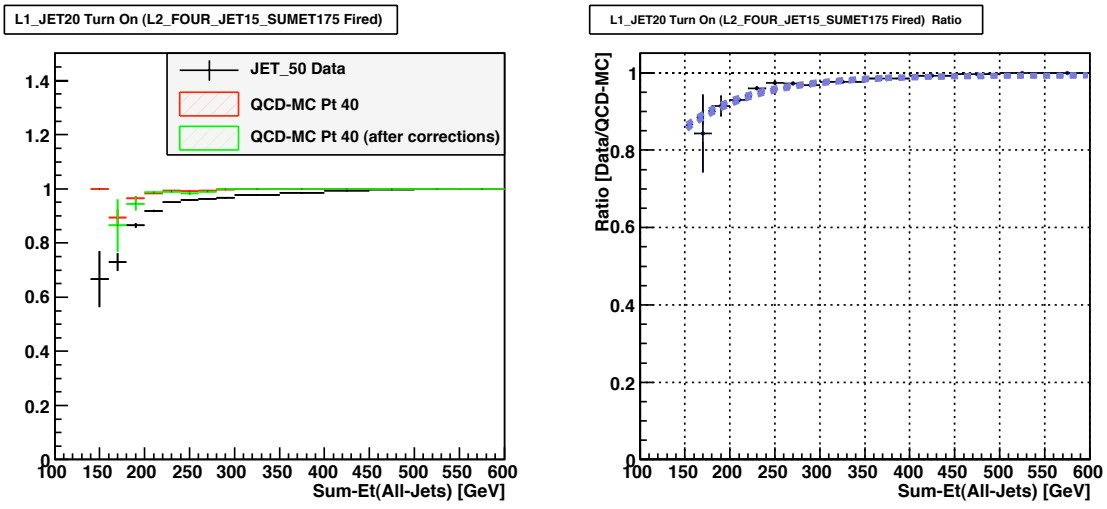

Figure 17: L1_JET20 Correction for L2-CONE : The left hand plot shows the turn-on for L1_JET20 for events which the standard event selection & passed the L2-CONE trigger. The right hand plot is the ratio of the trigger turn-ons of JET_50 data to QCD-MC Pt40(after correction). The dashed blue line is the fit to the ratio using equation 5.

7 VH_MULTIJET **Trigger**

The TOP_MULTI_JET trigger was originally designed to select all-hadronic $t\bar{t}$ events. Although it selects events with 4-jets, the L2-SumEt cut is high and this compromises the efficiency for Higgs events. The VH _MULTIJET was developed to address the inadequcies of TOP_MULTIJET. This trigger was designed to improve the acceptance for low-mass higgs events [4]. The definition of this trigger is:

Level-1 L1_JET20

Level-2 L2_THREEJET20_SUMET130

Level-3 NULL

The trigger turn-on measurement followed the same procedure outlined in section 6.1. The QCD-MC Pt40 was reweighed using the same reweigh matrix & ONLINE ENERGY SCALE used for the TOP_MULTI_JET_V-12 analysis. Figure 18 shows the VH_MULTIJET trigger turn-on for JET_50 data and QCD-MC Pt40 before and after corrections. The bottom row are the trigger turn on ratios of Data to corrected QCD-MC Pt40. The fitted ratio for VH_MULTIJET is 0.953 $\pm$ 0.004.

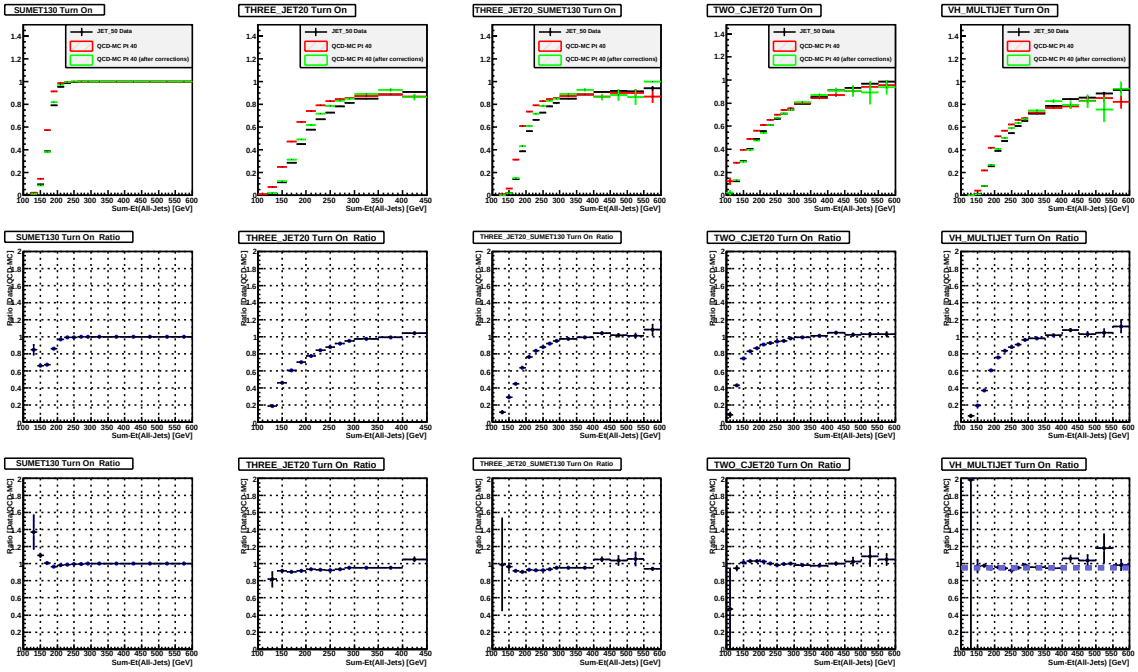

Figure 18: The trigger turn-on for VH_MULTIJET : The top row shows the L2 trigger trigger turn on for VH_MULTIJET and its components. The middle row shows the ratio of JET_50 data to QCD-MC(uncorrected). The bottom row shows the ratio of JET_50 data to QCD-MC(corrected). The fitted ratio for VH_MULTIJET is 0.953 $\pm$ 0.004.

The L1 trigger for VH_MULTIJET is L1_JET20. As for TOP_MULTI_JET triggers, the L1_JET20 trigger turn on for events passing the standard event selection & L2 component

of VH_MULTIJET is measured (figure 19). The ratio of the JET_50 to corrected QCD-MC Pt40 is fitted to equation 6.

$$f(x) = A\left(1 - \exp^{-Bx}\right) \tag{6}$$

x : Sum-Et(All-Jets)

After the fit, the parameters for the turn-on are:

A 0.9959 ± 0.0009

B 0.0144 ± 0.0002

The overall MC scale factor for VH_MULTIJET is $0.953 \times f(x)$ (as defined in equation 6).

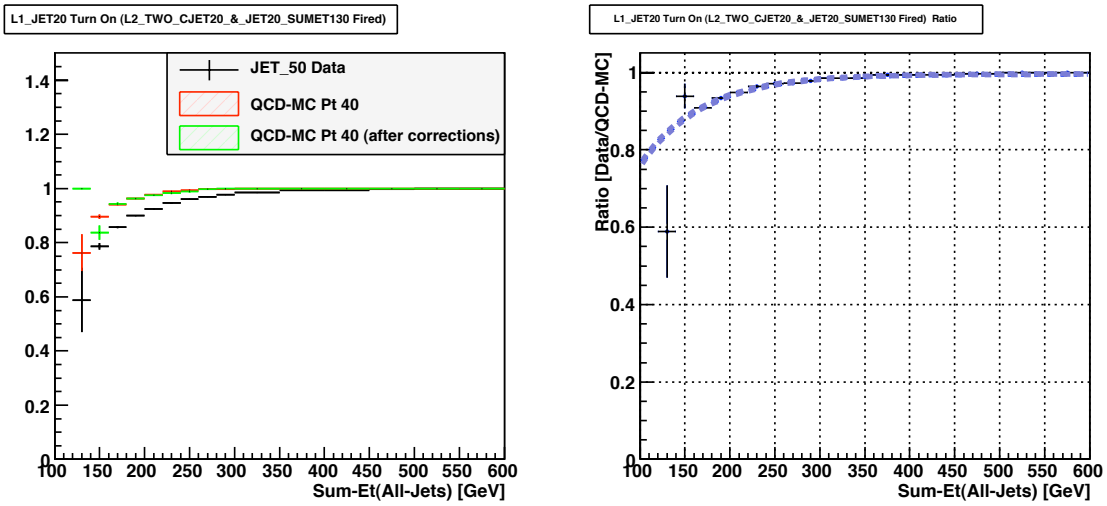

Figure 19: L1_JET20 correction for VH_MULTIJET : The left hand plot shows the turn-on for L1_JET20 for events which the standard event selection & passed the L2 component of the VH_MULTIJET trigger. The right hand plot is the ratio of the trigger turn-ons of JET_50 data to QCD-MC Pt40(after correction). The dashed blue line is the fit to the ratio using equation 6.

8 Systematic Errors

As a cross check of the measurements made, the trigger study was repeated with a different data set: JET_50 was replaced with JET_20 and QCD-MC Pt40 was replaced with QCD-MC Pt18. The events from these data sets were forced to pass the same standard event selection (section 3). The same reweigh matrices defined by equations 1 and 4 were used to reweigh the QCD-MC Pt18 to match the JET_20 data. As JET_20 and QCD-MC Pt18 have lower E_T cuts than JET_50 & QCD-MC Pt40, a smaller number of events survive the event selection. This had an effect on the reweigh matrix where a coarser binning had to be used. The reweighed QCD-MC Pt 18 distributions are shown in figures 20 and 21.

After the reweigh matrix, the same L2 cluster rescaling (table 1) was applied and the trigger turn on was measured. The trigger turn-ons for the TOP_MULTI_JET & VH_MULTIJET using JET_20 and QCD-MC Pt18 are shown in figures 22, 23 and 24. Again the QCD-MC Pt 18 trigger turn-ons started following the data after the corrections were applied. The MC scale-factor was remeasured by fitting the ratio of the trigger turn-ons of JET_20 data to corrected QCD-MC Pt 8. As there were few events at high SumEt, the final fits of the Data/MC ratio are restricted to the lower to mid SumEt region. From this alternative data-set, the fitted scale factors were:

- TOP_MULTI_JET_V-2-9 (PACMAN) : 0.930 $\pm$ 0.047 (when fitted $200 <$ Sum-Et(All-Jets) < 400 GeV
- TOP_MULTI_JET_V-12 (L2-CONE) : 1.006 $\pm$ 0.049 (when fitted $100 <$ Sum-Et(All-Jets) < 350 GeV
- VH_MULTIJET : 0.934 $\pm$ 0.024 (fitted over full Sum-Et(All-Jets) range)

The L1_JET20 turn-ons were also measured using the JET_20/QCD-MC Pt18 data sets and fitted to the same functions (equations 3, 5 and 6). Due to the low statistics of JET_20/QCD-MC Pt18 data, the errors on the fitted turn-ons are large. So all of the fitted turn-ons measured with JET_50/QCD-MC Pt40 data are compatible with the fitted functions from JET_20/QCD-MC Pt18 (figures 25, 26 and 27) . Table 4 summarises the measurements for this systematics cross-check.

The low statistics of the JET_20 data and QCD-MC Pt18 make it difficult to measure the true systematic differences. The error on the fitted parameters for L1_JET20 are large which make them compatible with the fits from the higher statistic JET_50/QCD-MC Pt40 data set. So there is no systematic for the L1_JET20 turn-on. The fitted ratios for the L2 Scale-factors measured with JET_50/QCD-MC Pt 40 and JET_20/QCD-MC Pt 18 agree each other to 4%. As a conservative estimate of the systematic, this 4% variation is taken as a measure of the trigger systematic.

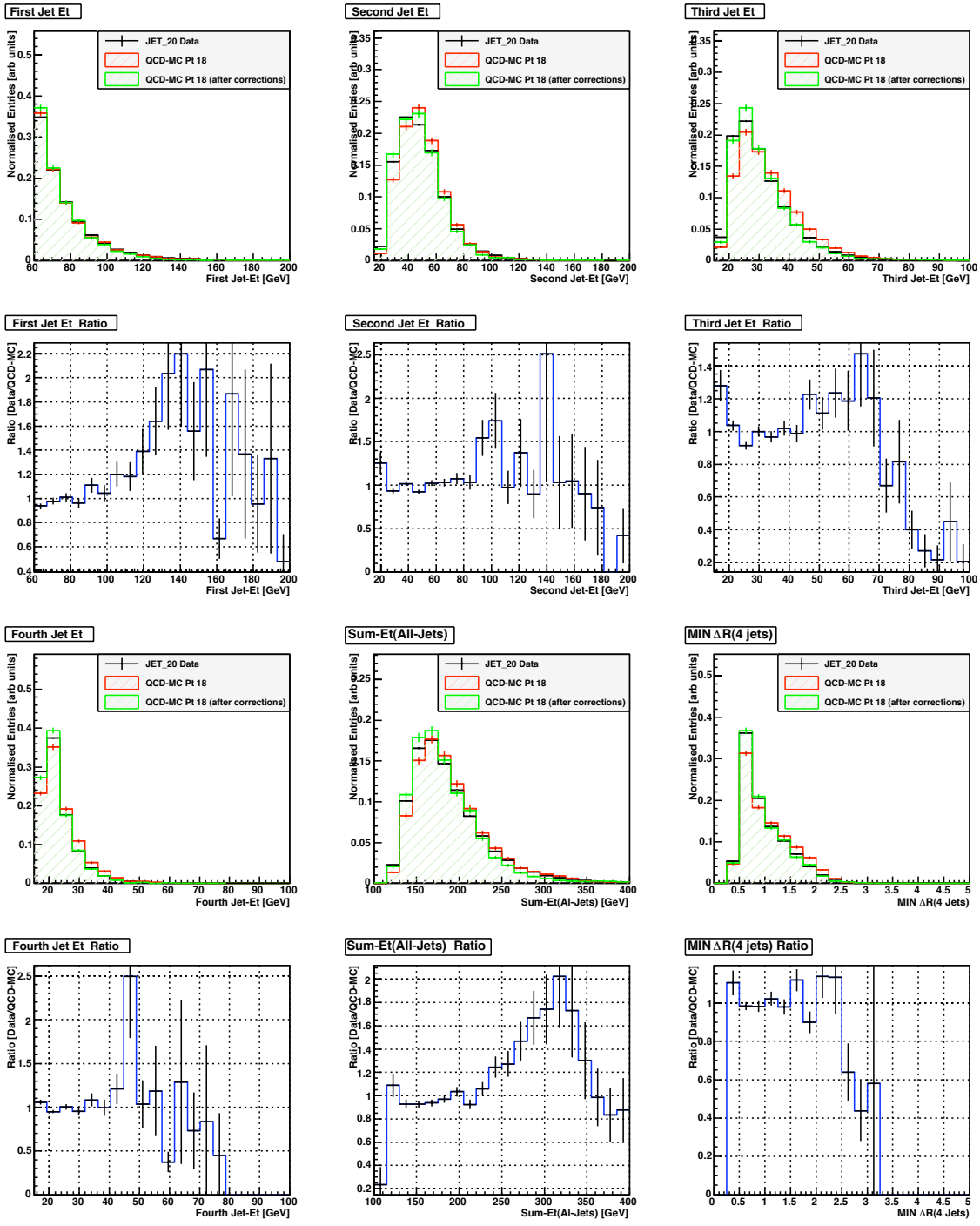

Figure 20: Jet-E_T , Sum-Et, MIN ΔR distributions for JET_20 data and QCD-MC Pt18 for PACMAN data. After applying the reweigh matrix, the corrected QCD-MC Pt18 (green) matches the JET_20 data (black) better.

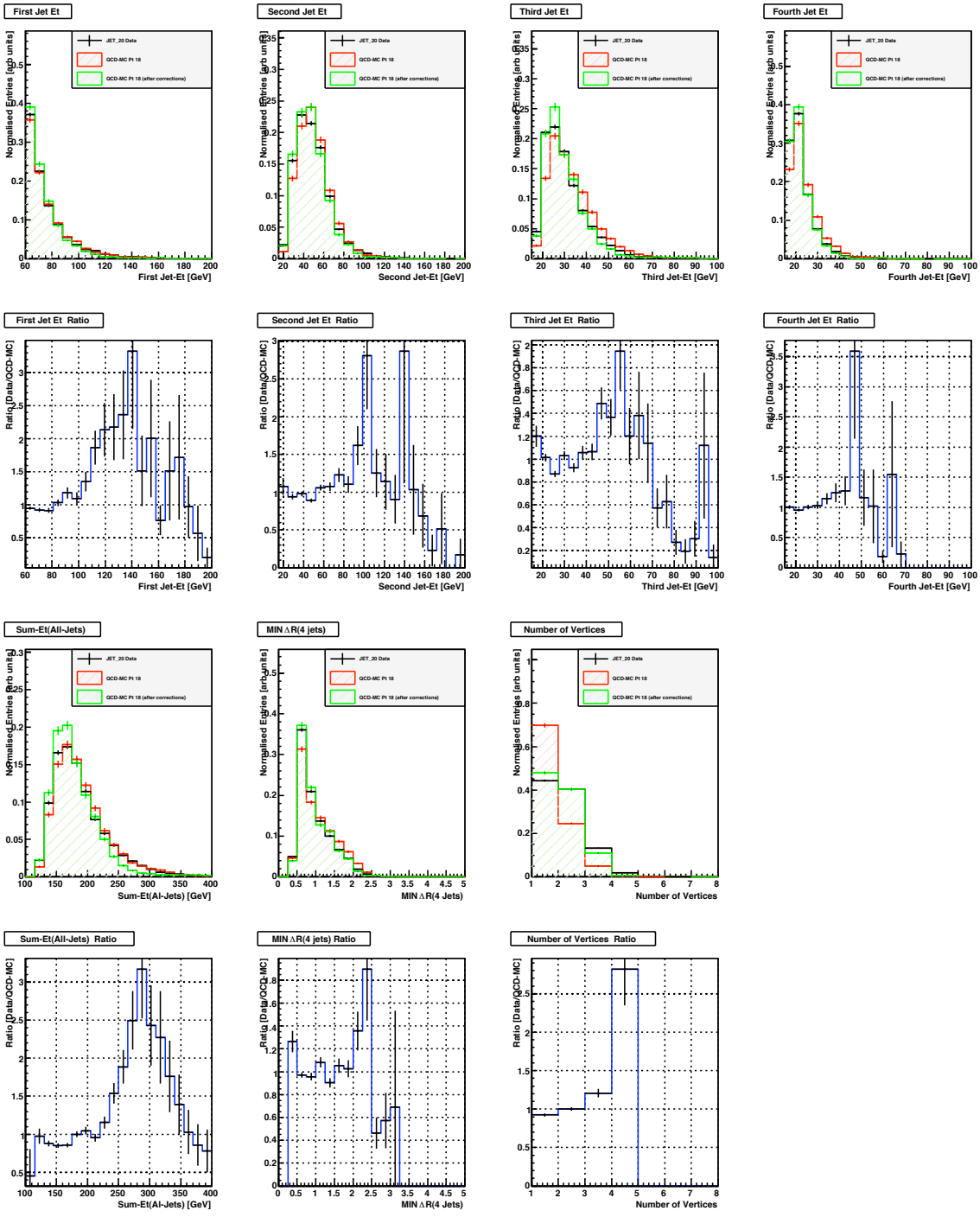

Figure 21: Jet-E_T , Sum-Et, MIN ΔR & N-Vertex distributions for JET_20 and QCD-MC Pt18 for L2-CONE data. After applying the reweigh matrix, the corrected QCD-MC Pt18 (green) matches the JET_20 data (black) better.

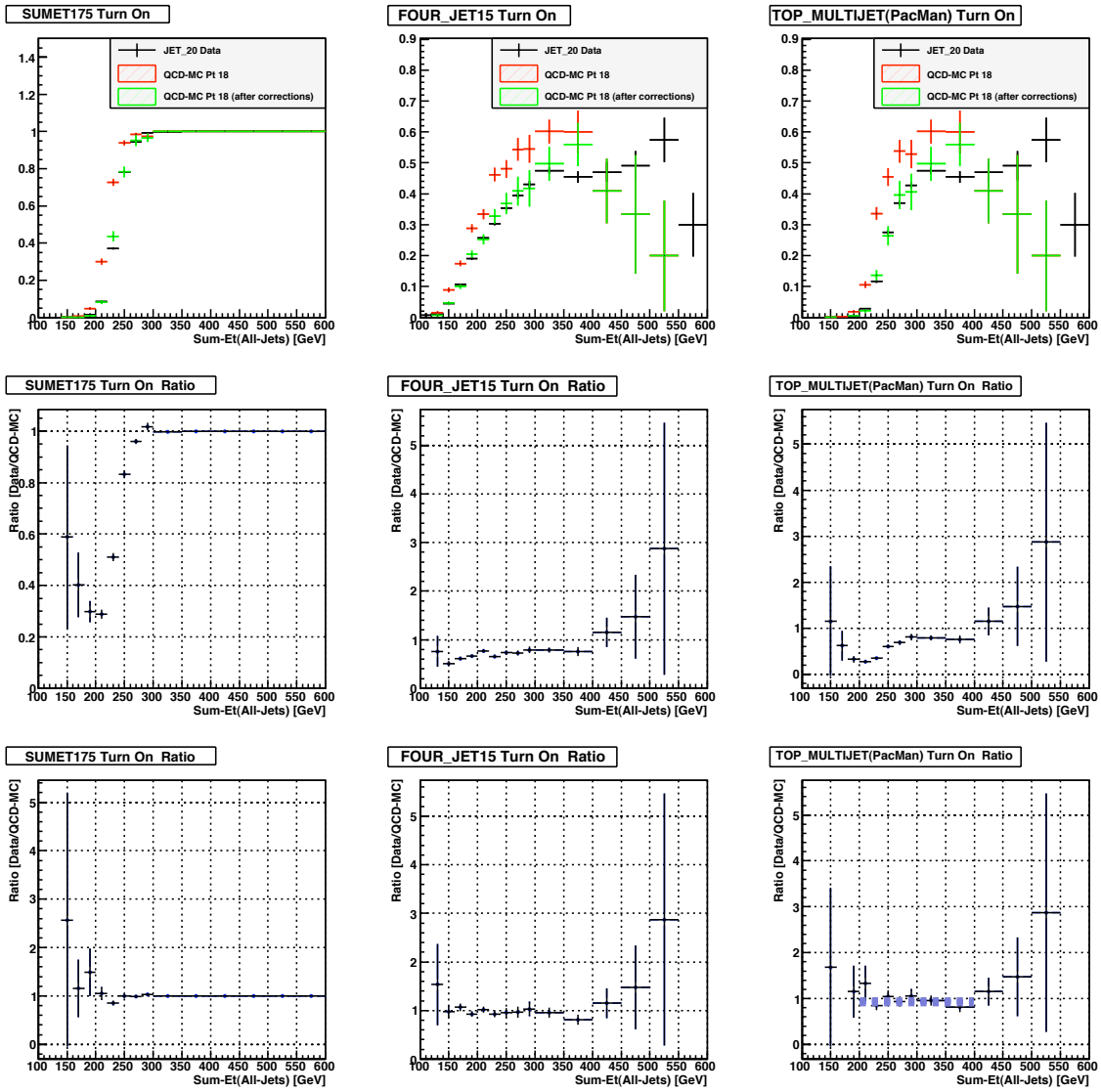

Figure 22: Trigger turn-on for TOP_MULTI_JET_V2-9 (PACMAN) as measured with QCD-MC Pt18 and JET_20 data. The middle row shows the ratio of trigger of JET_20 data to uncorrected QCD-MC Pt18. The bottom row are the trigger turn-on ratios of JET_20 data to corrected QCD-MC Pt18. After the QCD-MC is corrected, the ratio plots are flat. The fitted ratio of TOP_MULTI_JETfor the corrected QCD-MC Pt18 is 0.930 $\pm$ 0.047.

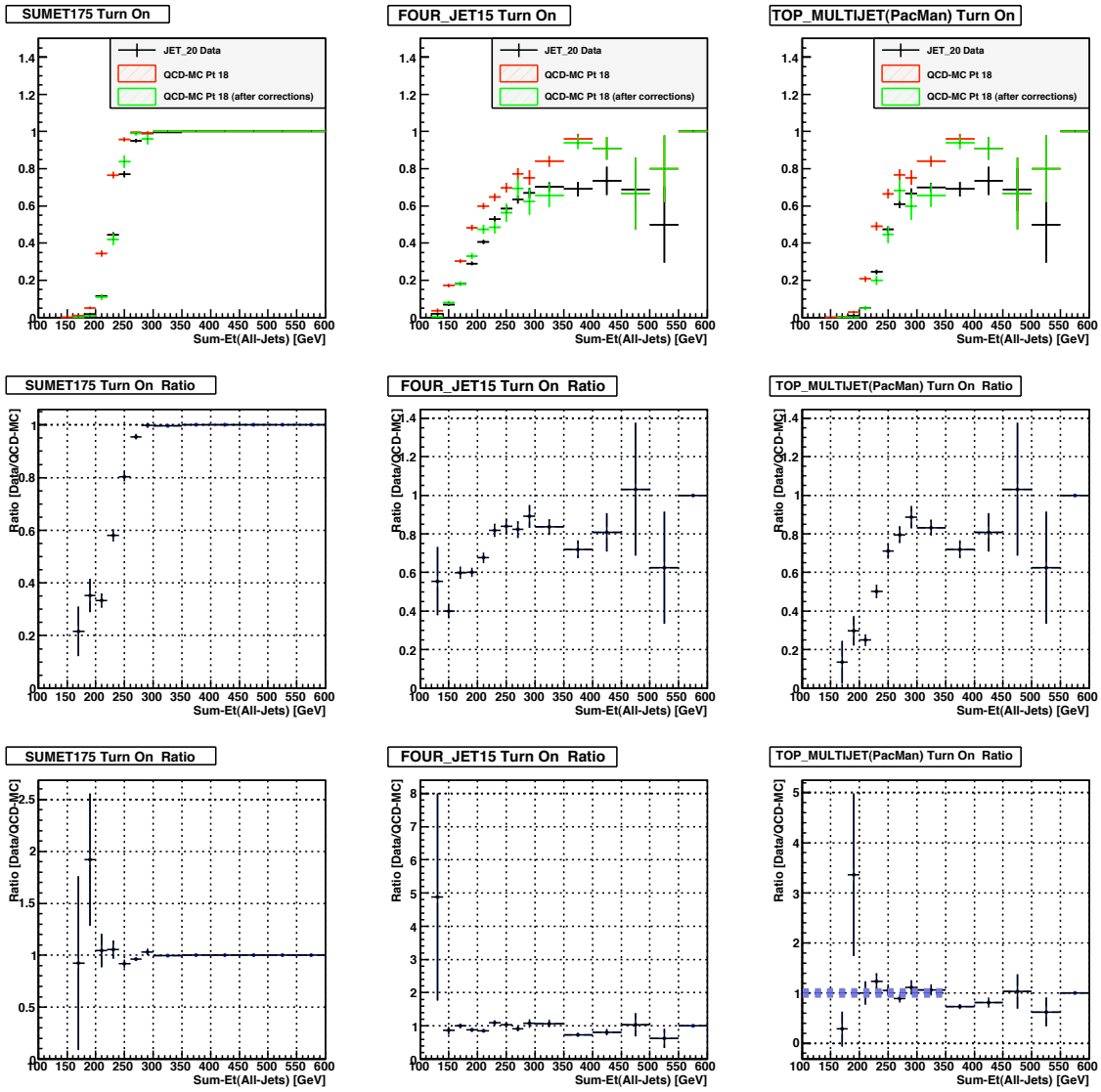

Figure 23: Trigger turn-on for TOP_MULTI_JET_V12 (L2-CONE) as measured with QCD-MC Pt18 and JET_20 data. The middle row shows the ratio of trigger of JET_20 data to uncorrected QCD-MC Pt18. The bottom row are the trigger turn-on ratios of JET_20 data to corrected QCD-MC Pt18. After the QCD-MC is corrected, the ratio plots are flat. The fitted ratio of TOP_MULTI_JETfor the corrected QCD-MC Pt18 is 1.006 ± 0.049.

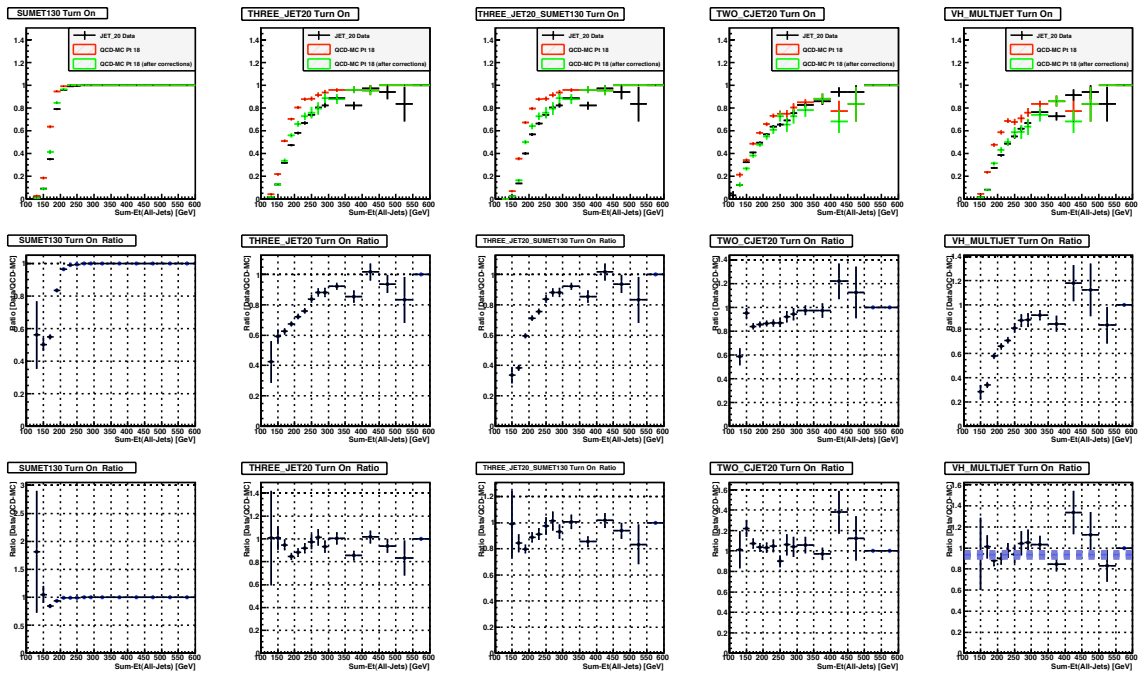

Figure 24: Trigger turn-on for VH_MULTIJET as measured with QCD-MC Pt18 and JET_20 data. The middle row shows the ratio of trigger of JET_20 data to uncorrected QCD-MC Pt18. The bottom row are the trigger turn-on ratios of JET_20 data to corrected QCD-MC Pt18. After the QCD-MC is corrected, the ratio plots are flat. The fitted ratio of VH_MULTIJET for the corrected QCD-MC Pt18 is 0.934 $\pm$ 0.024.

Table 4: MC trigger corrections as measured with JET_20 data and QCD-MC Pt18. The measured values are all compatible with the measurements taken with JET_50 data and QCD-MC Pt40. Only the fit for the L1 for TOP_MULTI_JET_v-9 differs. But the errors on the fitted parameters are large enough to be compatbile with the fitted function from JET_50 & QCD-MC Pt 40 (figure 20)

	L1 MC Scale Factor	L2 MC Scale Factor
TOP_MULTI_JET_v1-8	Not Needed	0.930 $\pm$ 0.047
TOP_MULTI_JET_v-9	$f(x) = A\left(1 - \exp^{-Bx}\right) + C$ $A = 4997.4 \pm 0.1$ $B = 0.0495 \pm 0.001$ $C = -4996.5 \pm 0.1$	0.930$\pm$ 0.047
TOP_MULTI_JET_v-12	$f(x) = A\left(1 - \exp^{-Bx}\right)$ $A = 1.041 \pm 0.101$ $B = 0.0085 \pm 0.0033$	1.006 $\pm$ 0.049
VH_MULTIJET	$f(x) = A\left(1 - \exp^{-Bx}\right)$ $A = 0.961 \pm 0.025$ $B = 0.017 \pm 0.006$	0.934 $\pm$ 0.024

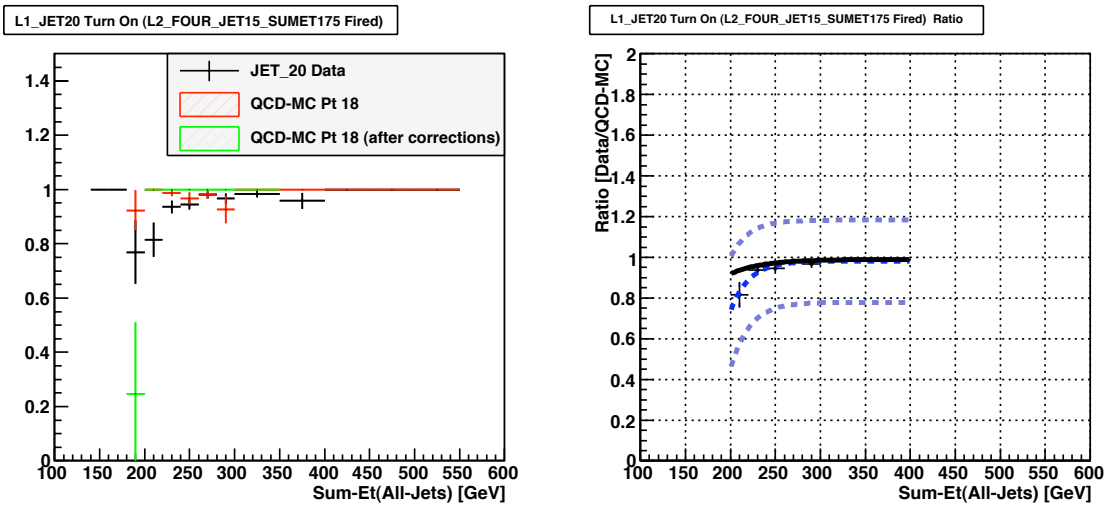

Figure 25: Measure of the L1_JET20 turn on for TOP_MULTI_JET_V-9 (PACMAN) using JET_20 data and QCD-MC Pt18. The left plot shows the measured turn-ons for events passing the L1_JET20 trigger if the L2 component of TOP_MULTI_JET_V-9 is true for JET_20 data and (un)corrected QCD-MC Pt 18. The right plot is the ratio of the JET_20 trigger turn-on to the corrected QCD-MC Pt 18. The lighter blue lines are $\pm 1\sigma$ variation of the fit parameters. The black line is the fit using JET_50/QCD-MC Pt40. This fit is compatible with the JET_20/QCD-MC Pt18 measurement.

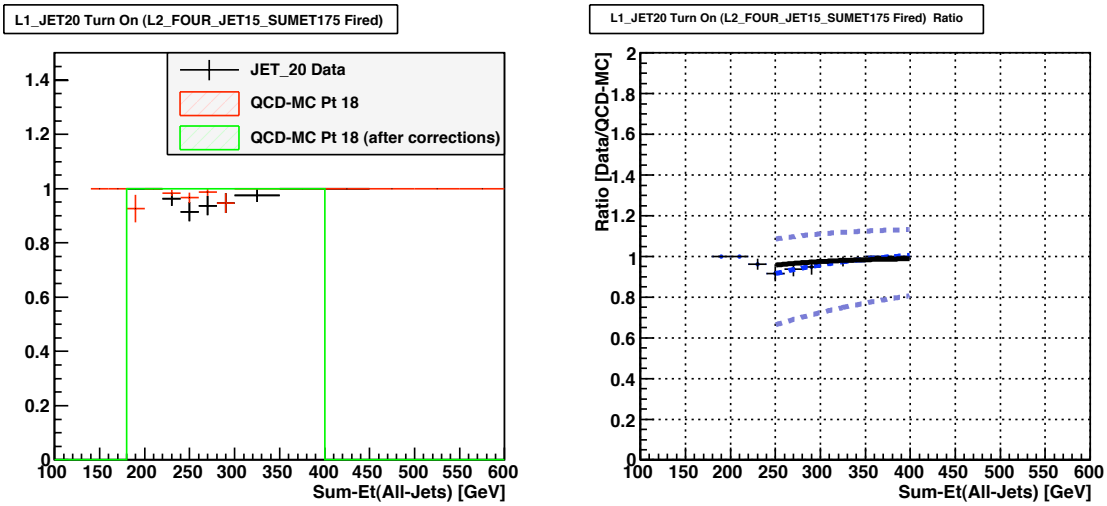

Figure 26: Measure of the L1_JET20 turn on for TOP_MULTI_JET_V-12 (L2-CONE) using JET_20 data and QCD-MC Pt18. The left plot shows the measured turn-ons for events passing the L1_JET20 trigger if the L2 component of TOP_MULTI_JET_V-12 is true for JET_20 data and (un)corrected QCD-MC Pt 18. The right plot is the ratio of the JET_20 trigger turn-on to the corrected QCD-MC Pt 18. The lighter blue lines are $\pm 1\sigma$ variation of the fit parameters. The black line is the fit using JET_50/QCD-MC Pt40. This fit is compatible with the JET_20/QCD-MC Pt18 measurement.

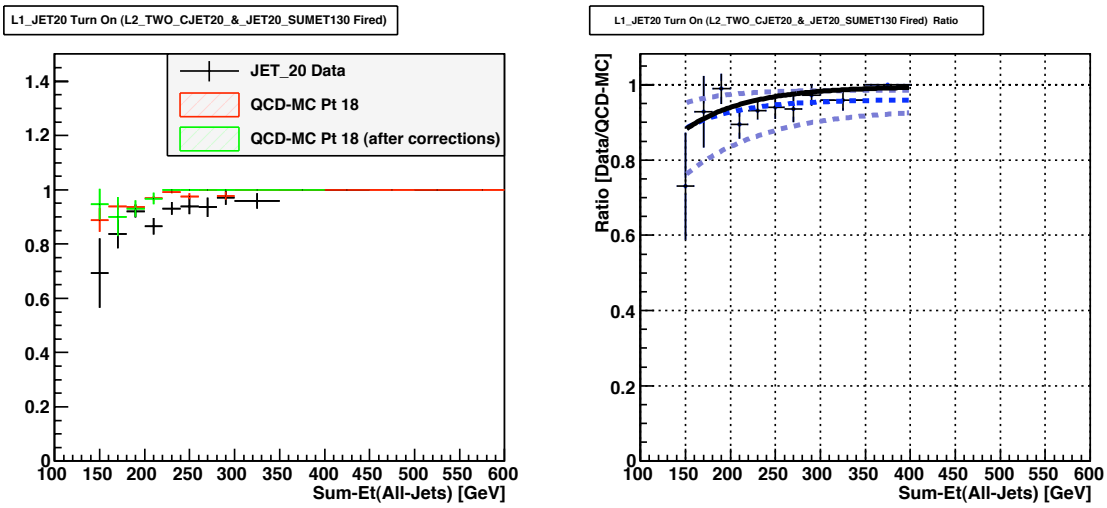

Figure 27: Measure of the L1_JET20 turn on for VH_MULTIJET (L2-CONE) using JET_20 data and QCD-MC Pt18. The left plot shows the measured turn-ons for events passing the L1_JET20 trigger if the L2 component of VH_MULTIJET is true. for JET_20 data and (un)corrected QCD-MC Pt 18. The right plot is the ratio of the JET_20 trigger turn-on to the corrected QCD-MC Pt 18. The lighter blue lines are $\pm 1\sigma$ variation of the fit parameters. The black line is the fit using JET_50/QCD-MC Pt40. This fit is compatible with the JET_20/QCD-MC Pt18 measurement.

9 Application to the Higgs Signal MC

The purpose of these trigger studies is to derive a set of generic corrections which can be applied to any MC sample to get a more correct trigger response. The MC corrections applied to the QCD-MC samples are applied to the Higgs signal MC. Only the reweigh matrix is not applied. We assume PYTHIA models the dynamics of a Higgs decay correctly. Thus the overall MC trigger weight is:

$$\text{Trigger Weight(Sum-Et)} = \text{Event Passes L2}\times\text{L1 MC Scale Factor(Sum-Et)}\times\text{L2 MC Scale Factor} \quad (7)$$

The L1 and L2 scale factors are summarised in table 5.

Table 5: L1 & L2 MC Scale Factors. The overall trigger weight is a product of the L1 MC Sale Factor and L2 MC Scale Factor. For the L1 MC Scale Factors, x is the Sum-Et(All Jets).

	L1 MC Scale Factor	L2 MC Scale Factor
TOP_MULTI_JET_v1-8	Not Needed	0.963 ± 0.008
TOP_MULTI_JET_v-9	$f(x) = A\left(1-\exp^{-Bx}\right)+C$ $A = 19.23 \pm 0.01$ $B = 2.80E-02 \pm 0.04E-02$ $C = -18.24 \pm 0.01$	0.963 ± 0.008
TOP_MULTI_JET_v-12	$f(x) = A\left(1-\exp^{-Bx}\right)$ $A = 0.994 \pm 0.001$ $B = 0.0132 \pm 0.0003$	0.973 ± 0.06
VH_MULTIJET	$f(x) = A\left(1-\exp^{-Bx}\right)$ $A = 0.9959 \pm 0.0009$ $B = 0.0144 \pm 0.0002$	0.953 ± 0.004

Using these trigger corrections, one can measure the acceptable for each trigger version (table 6), where the trigger acceptance is defined as:

$$\text{Trigger Acceptance} = \frac{\text{Passes event-selection \& Trigger fires}}{\text{Passes event-selection}} \quad (8)$$

The table shows the acceptance improved after the L2 clustering algorithm changed from PACMAN to L2-CONE and the new VH_MULTIJET makes further increases.

Table 6: Trigger acceptance for VBF, WH & ZH for 120 GeV Higgs and $t\bar{t}$. All the MC samples had the trigger corrections applied.

	VBF120	WH120	ZH120	$t\bar{t}$
TOP_MULTI_JET_v1-8	36.8%	21.7%	32.1%	64.5%
TOP_MULTI_JET_v-9	36.0%	21.3%	31.5%	63.5%
TOP_MULTI_JET_v-12	48.9%	33.3%	46.7%	69.5%
VH_MULTIJET	59.2%	57.4%	70.5%	82.7%

10 Conclusion

A set of corrections were derived for CDF-MC to improve the trigger simulation. The corrections applied to the MC are:

- Online Energy Corrections to correct the L2-Cluster energy
- MC Scale Function to correct the MC trigger turn-on to make it match data

The corrections for the L2-Cluster energy can be found in table 1 and the MC scale factors are in table 5. All the corrections were derived using JET_50 data and QCD-MC Pt 40. As a measure of the systematic error, the analysis was repeated using JET_20 data and QCD-MC Pt 18. Unfortunately a small number of events passed the event-selection & trigger requirements which made it difficult to have a true measure of the systematic error. The fits for the L1_JET20 turn-on agree between the two samples. The L2 scale factor has 4% variation. This 4% is taken as an estimate of the systematic error.

The focus of this study has been for the all-hadronic Higgs search. However the results should be applicable to other analysis using multi-jet trigger (eg: all hadronic top measurements). Also the technique developed in this not are applicable to other analysis where one must rely on MC & simulation to measure the trigger.

References

[1] Rong-Shyang Lu, Ankush Mitra, Song-Ming Wang, Aart Heijboer, Joe Kroll, and Daniel Whiteson. A search for the standard model higgs boson in the all-hadronic channel using a matrix element discriminant. CDF/ANAL/CDF/CDFR 9286, Academia Sinica and University of Pennsylvania and University of California,Irvine, April 2008.

[2] Rong-Shyang Lu, Ankush Mitra, Song-Ming Wang, Aart Heijboer, Joe Kroll, and Daniel Whiteson. Study of the top multijet trigger efficiency for the search of the standard model higgs boson in the all hadronic channel. CDF/ANAL/CDF/CDFR 9252, Academia Sinica and University of Pennsylvania and University of California,Irvine, March 2008.

[3] M. Casarsa M. Convery G. Cortiana M. Dell'Orso G. Flanagan H. Frisch P. Gianetti O. Gonzalez A. Gresele M. Jones T. Liu D. Lucchesi M. Piendibene L. Ristori L. Rogondino V. Rusu L. Sartori S. Torre Y. Tu V. Veszpremi M. Vidal S.M. Wang A. Bhatti, A. Canepa. Proposal for level-2 calorimeter trigger upgrade. CDF/DOC/TRIGGER/CDFR/ 8415, The Rockefeller University, University of Pennsylvania , INFN Trieste, INFN Padova, INFN Pisa, Purdue University, University of Chicago, CIEMAT (Madrid), Fermi National Accelerator Laboratory, INFN Frascati, Academia Sinica, 13 September 2006.

[4] Yen-Chu Chen, Ankush Mitra, Shang-Yuu Tsai, Song-Ming Wang, and Rong-Shyang Lu. New multijet trigger. CDF/PHYS/TRIGGER/CDFR 9326, Institute of Physics, Academia Sinica, Taiwan and Department of Physics, National Taiwan University, Taiwan, 15 May 2008.

[5] Joint physics meeting. WebTalks, 27 May 2009.